www.the-innovation.org

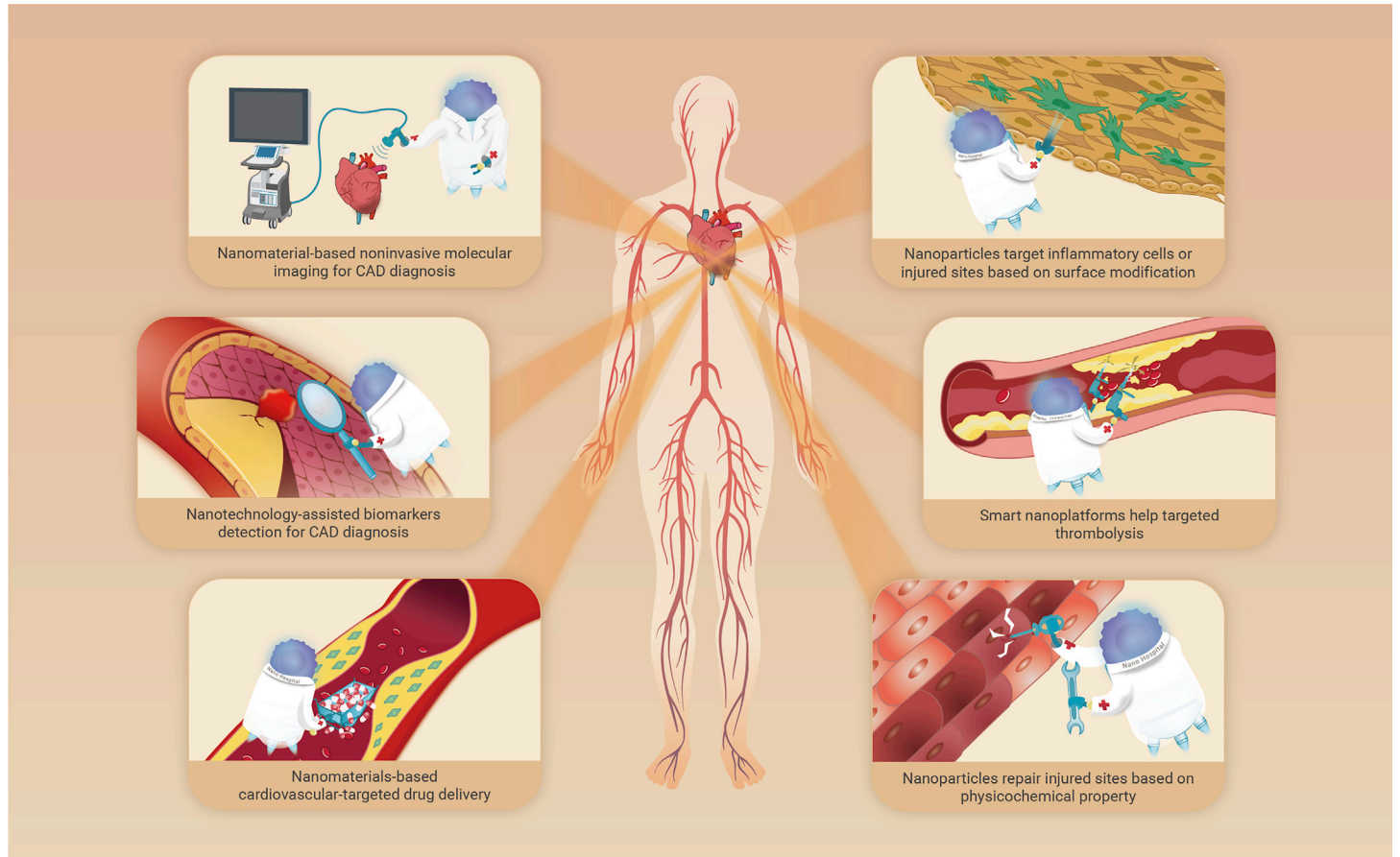# Nanotechnology for cardiovascular diseases

Qinqin Hu,[1,2,3] Zheyan Fang,[1,3] Junbo Ge,[1,2,*] and Hua Li[1,2,*]

*Correspondence: ge.junbo@zs-hospital.sh.cn (J.G.); lihua199988@hotmail.com (H.L.)

GRAPHICAL ABSTRACT

PUBLIC SUMMARY

- Nanotechnology represents new viable approaches for diagnosis and treatment of cardiovascular diseases, the leading cause of morbidity and mortality worldwide

- Nanotechnology-assisted biosensing and molecular imaging can improve the sensitivity and specificity in the diagnosis of cardiovascular diseases

- Nanomaterials enable targeted drug delivery or directly exert therapeutic action for cardiovascular system, based on their physicochemical properties and surface modification

Nanotechnology for cardiovascular diseases

Qinqin Hu,[1,2,3] Zheyan Fang,[1,3] Junbo Ge,[1,2,*] and Hua Li[1,2,*]

[1]Department of Cardiology, Shanghai Institute of Cardiovascular Diseases, Shanghai Xuhui District Central Hospital & Zhongshan-xuhui Hospital, Zhongshan Hospital, Fudan University, Shanghai 200032, China
[2]Institutes of Biomedical Sciences, Fudan University, Shanghai 200032, China
[3]These authors contributed equally
*Correspondence: ge.junbo@zs-hospital.sh.cn (J.G.); lihua199988@hotmail.com (H.L.)

Cardiovascular diseases have become the major killers in today's world, among which coronary artery diseases (CADs) make the greatest contributions to morbidity and mortality. Although state-of-the-art technologies have increased our knowledge of the cardiovascular system, the current diagnosis and treatment modalities for CADs still have limitations. As an emerging cross-disciplinary approach, nanotechnology has shown great potential for clinical use. In this review, recent advances in nanotechnology in the diagnosis of CADs will first be elucidated. Both the sensitivity and specificity of biosensors for biomarker detection and molecular imaging strategies, such as magnetic resonance imaging, optical imaging, nuclear scintigraphy, and multimodal imaging strategies, have been greatly increased with the assistance of nanomaterials. Second, various nanomaterials, such as liposomes, polymers (PLGA), inorganic nanoparticles (AuNPs, MnO$_2$, etc.), natural nanoparticles (HDL, HA), and biomimetic nanoparticles (cell-membrane coating) will be discussed as engineered as drug (chemicals, proteins, peptides, and nucleic acids) carriers targeting pathological sites based on their optimal physicochemical properties and surface modification potential. Finally, some of these nanomaterials themselves are regarded as pharmaceuticals for the treatment of atherosclerosis because of their intrinsic antioxidative/anti-inflammatory and photoelectric/photothermal characteristics in a complex plaque microenvironment. In summary, novel nanotechnology-based research in the process of clinical transformation could continue to expand the horizon of nanoscale technologies in the diagnosis and therapy of CADs in the foreseeable future.

INTRODUCTION

Cardiovascular diseases (CVDs) are the leading cause of morbidity and mortality in both the developed and developing world.[1,2] With an estimated 17.9 million deaths annually, CVDs contribute 32% of all global deaths, of which 85% are due to heart attack or stroke.[3,4] The most common cause of CVDs is atherosclerosis, a progressive disease involving the deleterious accumulation of lipids and fibrins within the arterial wall and a maladaptive immune response and dysregulation of cholesterol metabolism, initiating the formation of atherosclerotic plaques. The branches off the aortic root, namely, the left and right coronary arteries, supply oxygen-rich blood to the myocardium. Atherosclerotic lesions in the coronary arteries can cause lumen obstruction and stenosis, resulting in myocardial ischemia, hypoxia, and even necrosis, known as coronary atherosclerotic heart diseases or coronary artery disease (CADs).[5]

In addition to effective control of cardiovascular risk factors, early diagnosis is crucial to prevent CADs.[6] Thanks to innovations in modern technology and the discovery of related biomarkers, there have been considerable advances in diagnostic methods in clinical practice, such as electrocardiography (ECG) and imaging techniques to evaluate abnormal cardiovascular conditions.[7,8] In clinical treatment, medication can improve the long-term prognosis and prevent acute cardiovascular events. For example, evidence-based pharmacotherapies such as β-blockers, lipid-lowering drugs, ACE inhibitors, angiotensin receptor blockers, and low-dose aspirin are recommended in clinical guidelines for long-term secondary prevention.[9] Moreover, the ischemia caused by thrombotic occlusion in acute cardiovascular events such as acute myocardial infarction (AMI) can be rescued by timely recanalization via thrombolytic therapy, stent implantation, or conventional recanalization surgery such as coronary artery bypass grafting.[10] With advances in the understanding of CADs, increasing numbers of clinical approaches and preclinical studies have continued to be used to prevent or delay myocardial dysfunction in recent decades. However, the high mortality rates of

CADs and consequent heart failure indicate that the current diagnosis and treatment methods still face great challenges.[11]

Compared with bulk materials, nanomaterials have a high ratio of surface area to volume as well as tunable optical, electronic, magnetic, mechanical, catalytic, thermal, and biological properties, and they can be engineered to have different sizes, shapes, chemical compositions, surface modifications, and hollow or solid structures. These properties enable researchers to design novel diagnostic and therapeutic platforms at the molecular level that can outperform traditional modalities.[12] In this review, based on summarizing the traditional diagnosis and treatment methods (Document S1), we first introduce the recent advances in the use of nanomaterials for the accurate diagnosis of CADs. Then, we provide a brief overview of the targeting strategies for nanomaterials to specifically recognize pathological sites, followed by a detailed summary of cutting-edge research on nanomaterial-based drug delivery systems and targeting inhibitors for the treatment of CVDs.

NANOTECHNOLOGY APPROACHES TO DETECT CADs
Nanotechnology-based approaches to detect CAD biomarkers

The early diagnosis of CADs increases the chance for successful treatment and potential cure, giving patients better prognoses and extended survival times. CAD-related biomarkers, such as cardiac troponins (cTns), myoglobin (Myo), creatinine kinase MB (CK-MB), C-reactive protein (CRP), and a series of miRNAs, are released into the bloodstream when the heart is damaged or stressed.[13] Therefore, one promising approach for the early diagnosis of CADs is to develop precise, specific, simple, stable, and rapid analyses of blood for such molecules. Mass spectrometry is frequently used for identifying potential biomarkers of CADs but is limited by sensitivity and specificity due to the low levels of biomarkers in human plasma. In view of these reasons, combining nanotechnologies with biosensors might serve as a promising solution for the diagnosis of early-stage CADs. The former can provide high-affinity binding to targeted molecules and reduce nonspecific adsorption via surface modification or structure optimization; the latter consists of two parts: a biological sensing element for recognizing targets and a transducer for converting data into electrical signals.[14] In this article, Tables 1 and S1 summarize biosensing methods for the rapid detection of important biomarkers with the assistance of nanomaterials.

Protein targets are first sensed by recognition molecules such as antibodies, aptamers, or molecularly imprinted polymers, and the sensing is then quantitatively detected by various methods, including electrochemistry (EC), electrochemiluminescence (ECL), fluorescent methods (FL), colorimetry, surface-enhanced Raman scattering (SERS), and surface plasmon resonance technology (SPR).[33] Nanomaterials with excellent optoelectronic properties greatly improve the detection sensitivity by orders of magnitude.[21,34–38] With ZnSnO$_3$ perovskite nanomaterial-decorated glassy carbon electrodes, Singh et al. designed a label-free EC biosensor to detect TnT.[39] This method exhibited subfemtomolar detection sensitivity owing to the ferroelectric property of ZnSnO$_3$. Another similar example is the use of a gold triangular nanoprism (AuTNP)-based localized SPR biosensor to monitor cTnT in plasma, serum, and urine. The cTnT assay achieved an attomolar (~15 a.m.) limit of detection (LOD), making it at least 50-fold more sensitive than other label-free techniques.[40] The shape of nanomaterials is another of the key features to optimize for sensitive detection. El-Safty et al. designed a label-free SERS sensor composed of 3D silver anisotropic nano-pinetree array-modified indium tin oxide (Ag NPT/ITO) substrates for the detection of Myo.[23] Ag NPT/ITO displayed the highest SERS performance among nanostructure shapes (nanoaggregates, nanorods, and nanobranches), which was attributed to the presence of numerous hotspots, particularly in the junctions between the central rod and side

Table 1. Nanotechnology-based biosensors to detect biomarkers of CADs

Biomarkers	Recognition elements	Nanomaterials	Methods	Linear range	LOD	Time (min)	Samples	Ref
Cardiac troponins(cTns)	antibody	AuNP-Hep-xGnP	DPV	0.050−0.35 ng/mL	0.016 ng/mL	20	whole blood	[15]
		Au NPs@CO-Fs	EC	0.5 pg/mL ∼ 10 ng/mL	0.17 pg/mL	—	whole blood	[16]
		Ag/CoS nanoflawors	ECL	0.1 fg/mL ∼ 100 pg/mL	0.03 fg/mL	—	human serum	[17]
		GPRu−Au, Au−CNN	ECL	10 fg/mL ∼ 10 ng/mL	3.94 fg/mL	—	human serum	[18]
	aptamer	DNA nanotetrahedron and MOF	EC	0.05−100 ng/mL	16 pg/mL	—	human serum	[19]
		DNA nanotetrahedron and Fe$_3$O$_4$/PDDA/Au@Pt	EC	0.01−100 ng/mL	7.5 pg/mL	—	human serum	[20]
		AuNPs	EC	100 a.m.−10 p.m.	100 a.m.	—	PBS	[21]
	MIP	boron nitride QDs	CV, EIS	0.01−5.00 ng/mL	5 pg/mL	—	human plasma	[22]
Myoglobin	antibody	Ag NPT/ITO	SERS	10 ng/mL ∼ 5 μg/mL	10 ng/mL	—	buffer, urine	[23]
		Pt-staining AuNPs	colorimetry	5.74−150 ng/mL	5.47 ng/mL	—	human serum	[24]
		UCNPs	FL-LFA	0.5−400 ng/mL	0.21 ng/mL	10	clinical samples	[25]
	aptamer	AuNPs/BNNSs	EC	0.1−100 μg/mL	34.6 ng/mL	—	human serum	[26]
CK-MB	antibody	polypyrrole@Bi$_2$WO$_6$	PEC	0.5−2000 ng/mL	0.16 ng/mL	—	human blood	[27]
Multitargets	antibody (cTnI, CRP)	TiO$_2$ nanofibrous	ELISA	10 pg/mL ∼ 100 ng/mL 1 pg/mL ∼ 100 ng/mL	37 pg/mL 0.8 pg/mL	30	spiked in whole blood	[28]
	aptamer (Myo, cTnI)	HsGDY@NDs	EIS	10 fg/mL ∼ 1 ng/mL 10 fg/mL ∼ 100 ng/mL	9.04 fg/mL 6.29 fg/mL	—	human serum	[29]
miRNAs	complementary strands	hollow Ag/Au NS	SERS with CHA	1 fM ∼ 10 nM	0.306 fM	—	human blood	[30]
		AuNPs@G4-SNAzyme	ECL with CHA	1 fM ∼ 1 nM	0.4 fM	—	human serum	[31]
		G4/MOFzymes	CL	10 a.m.−10 p.m.	2.17 a.m.	1	human serum	[32]

DPV (differential pulse voltammetry); EC (electrochemistry); ECL (electrochemiluminescence); CL (chemiluminescence); PEC (photoelectrochemistry); CV (cyclic voltammetry); EIS (electrochemical impedance spectroscopy); MIP (molecular imprinted polymer); LFA (lateral flow assay); CHA (chain hybridization amplification); SERS (surface-enhanced Raman spectroscopy); SNAzyme (spherical nucleic acid enzymes).

arms. Dual-hybrid or multihybrid nanostructure materials can inherit the advantages of multiple structures, successfully achieving signal amplification.[17,26,41] Ren's group proposed an ultrasensitive sandwich-type electrochemical immunosensor with TiO$_2$-PPy-Au as the substrate material and TB-Au-CO-Fs as signal labels for the quantitative detection of cTnI.[16] With the help of hybrid nanomaterials to improve electron transfer, the above sensor showed a linear range from 0.5 pg/mL to 10.0 ng/mL and a low LOD of 0.17 pg/mL. Besides, CdTe@IRMOF-3@CdTe nanocomposites also enlarge cTnI detection signals (Figure 1A).[42]

Because of the high surface area to volume ratio, nanomaterials, especially those with porous structures, are able to load large amounts of recognition elements (such as antibodies or aptamers) and transducer elements, resulting in signal cascade amplification.[19,23,29,43] Accordingly, Zhang et al. prepared nanodiamond hybrid hydrogen-substituted graphdiyne (HsGDY@NDs) to fabricate electrochemical aptasensors for detecting Myo and cTnI (Figure 1B).[29] Similar research was reported by Zhao et al., who synthesized Pd@Au nanocube-doped three-dimensional porous graphene to establish an ultrasensitive electrochemical immunosensor for detecting cTnI.[45] This nanostructure displayed good capture capability targeting antibodies and accelerated the electron transfer process on the electrode surface. Another method to increase of detection sensitivity is to modify nanomaterials with more signal transducer elements. Ru(bpy)$_3^{2+}$-loaded mesoporous silica nanoparticles (RMSNs) constructed according to this principle showed strong ECL signals, significantly outperforming conventional fluorescence detection (>3 orders of magnitude) (Figure 1C).[43] Similarly, Zhang et al. used magnetic Fe$_3$O$_4$ nanoparticles as nanocarriers to load large amounts of natural horseradish peroxidase (HRP), HRP-mimicking Au@Pt nanozymes, and G-quadruplex/hemin DNAzyme, which generated markedly enhanced EC signals because of the cocatalytic effects of the various enzymes.[20] In addition, the replacement of bioenzymes with nanozymes could not only ensure high sensitivity but also further improve the repeatability and stability of assays for clinical samples.[19,46]

Recently, nanotechnology-based multimodel or multi-target and point-of-care testing (POCT) assays have emerged for detecting CAD biomarkers, helping to assess the disease process more accurately, rapidly, and conveniently.[18,24,25,28,44,46−52] Previous studies found that ratiometric ECL could eliminate environmental interference and allow precise measurement. Yang's group prepared AuNP-modified graphitic phase carbon nitride nanosheets (Au-CNNs) that acted as donors, which matched well with the adsorption of acceptor GPRu-Au (AuNP-loaded graphene oxide/polyethylenimine) and ultimately showed high stability and a low LOD (Figure 1D).[18] In addition, to achieve simultaneous detection in different periods of AMI, a microfluidic paper-based device (μPAD) was designed by Khor et al. to detect glycogen phosphorylase isoenzyme BB (GPBB, early stage of ischemic myocardial injury within first 4 h), cTnT, and CK-MB (6 h after the onset of chest pain) (Figure 1E).[44] Moreover, due to its low cost, user-friendliness, time savings, and simplicity, POCT plays an important role in improving the quality of medical services and meeting the healthcare needs of remote districts. At present, a series of POCT methods have been designed to detect CAD biomarkers with the help of paper-based or microfluid portable devices and the signal amplification features of nanomaterials (such as ZnO nanowires, Au@AgPtNPs, core-shell upconversion nanoparticles, and TiO$_2$ nanofibers).[24,25,28,47] It has been noted that the time from collecting blood samples to the readouts of detection results can be less than 20 min. Regrettably, POCT methods currently still have LODs in the ng/mL range, which needs to be improved further.

In addition to protein biomarkers, noncoding RNAs, especially microRNAs (such as miR-133a and miR-499), are proposed to be novel biomarkers of myocardial injury.[13] Li's laboratory has made outstanding contributions in the
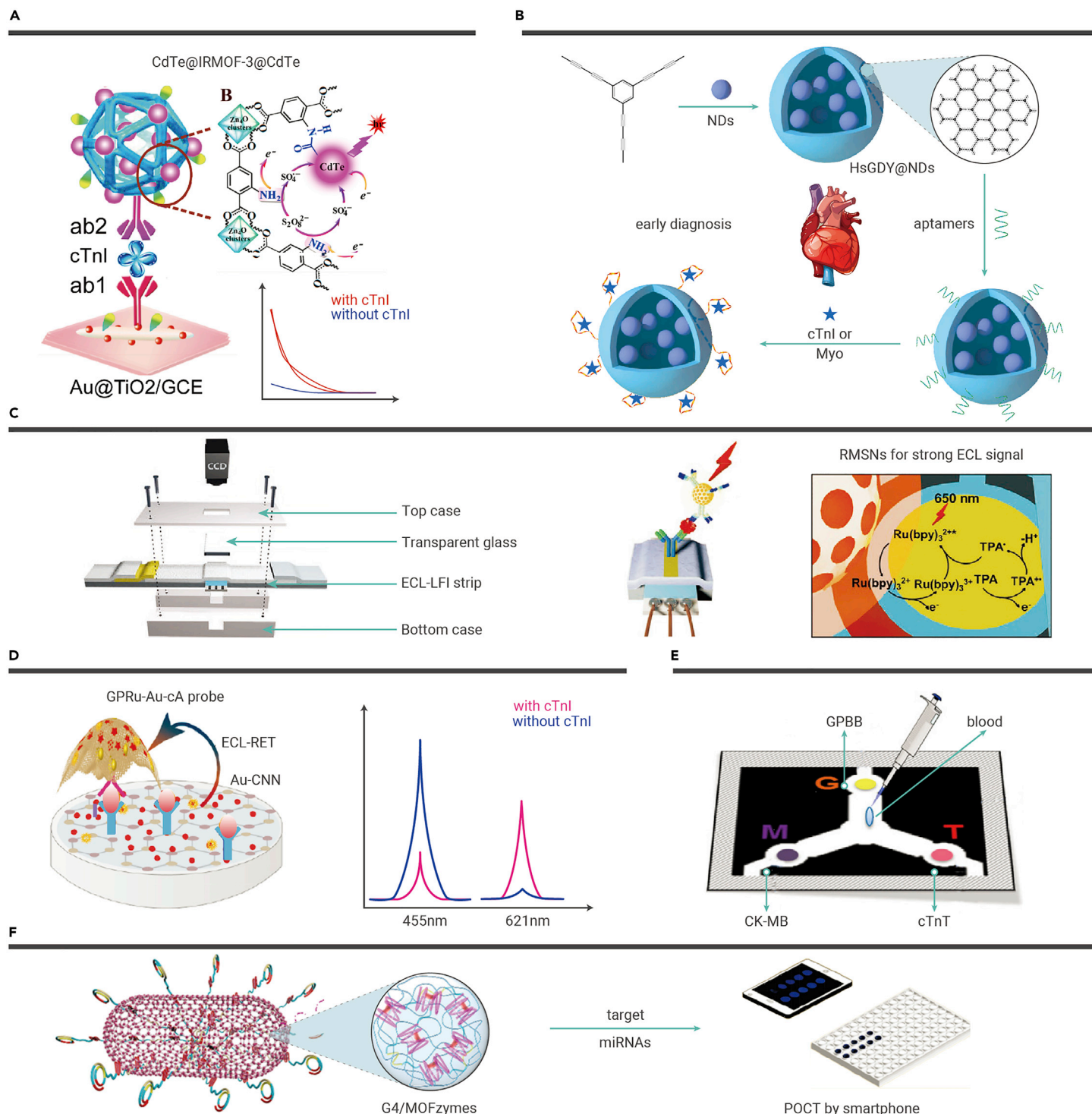
Figure 1. Schemes of nanotechnology-based biosensors for detection of CADs biomarkers (A) CdTe@IRMOF-3@CdTe nanocomposites to enlarge ECL signals.[42] The strong ECL emission was achieved from isoreticular metal-organic framework (IRMOF) accelerator enriched quantum dots (CdTe), which were applied as an efficient ECL signal tag for trace cTnI detection. IRMOF allowed for encapsulating large amounts of CdTe, and functioned as a novel coreactant accelerator for promoting the conversion of S_2O8^{2-} into $SO_4^{\bullet-}$, further boosting the ECL emission of CdTe. IRMOF@CdTe-based immunosensor eventually performed a wide response range from 1.1 fg/mL to 11 ng/mL and a very low detection limit (0.46 fg/mL) (copyright American Chemical Society, 2018). (B) HsGDY@NDs-based aptasensors for detecting Myo and cTnI.[29] The large surface and porous structure of HsGDY@NDs could absorb larger amounts of aptamer strands, giving low detection limits of 6.29 and 9.04 fg/mL for Myo and cTnI, respectively (copyright Elsevier Ltd., 2021). (C) Construction of RMSNs-based ECL-LFI strip for rapid, portable, and sensitive diagnosis.[43] The RMSNs-based ECL-lateral flow immunosensor (ECL-LFI) enabled highly sensitive detection of cTnI-spiked human serum within 20 min at femtomolar levels ($\approx$ 0.81 pg/mL) (copyright Wiley-VCH, 2020). (D) Ratiometric ECL-RET double-model detection of cTnI.[18] Based on nano-materials' features, a dual-wavelength ratiometric ECL resonance energy transfer (ECL-RET) sensing platform was developed for the detection of cTnI, showing high stability and low LOD (3.94 fg/mL) (copyright American Chemical Society, 2019). (E) uPAD for multi-target detection.[44] With advantages of stability and sensitivity, the nanomaterials, including AuNPs, AgNPs, and gold urchin NPs, were used as optical labels to provide visible color signals (copyright Elsevier Ltd. 2019). (F) Increase of catalytic activity with G4/MOFzymes for POCT of target miRNAs.[32] The interfaced G4 DNAzymes on MOFs (G4/MOFzymes) were produced by targeting miRNA-triggered rolling circle amplification (RCA) reactions, which displayed an about 100-fold higher catalytic activity than those in solution. By using the G4/MOFzyme catalysts in the luminol/H_2O_2 CL system, sensitive detection of myocardial infarction (AMI)-related two miRNAs (low to 1 fM seen with naked eyes) was achieved in human serum with a smartphone as a portable imaging detector (copyright American Chemical Society, 2020).

Table 2. Nanomaterial-based noninvasive molecular imaging for the diagnosis of CADs

Imaging modality	Nanoprobes	Sizes and shapes	Functions of nanoprobes	Targeting moieties	Targeted molecules/cells	Information provided	Ref
MRI	Gd-TPP$_{1880}$/LMWF$_{8775}$ CNPs	~240 nm, spheric	P-selectin targeting, cell penetrating, and Gd-DTPA loading	LMWF	P-selectin on activated ECs and platelets	visualization of inflammatory endothelial cells	[55]
Optical imaging	Ag$_2$S-AngII	~10 nm spheric	NIR-II fluorescence signals, loading AngII for high targeting MI in minutes	AngII	AT1R in MI tissues	visualization of hearts damaged after MI and ischemic myocardial tissues	[56]
Nuclear scintigraphy	^{64}Cu-CANF-comb	~16 nm, comb-like	loading ^{64}Cu for PET imaging, high targeting	CANF	NPRC	assessing the pathological function of NPRC and vulnerability of plaques	[57,58]
PAI	PBD-CD36 NPs	~50 nm, spheric	providing PA signals and high targeting	CD36 antibody	inflammatory cells	reflecting the inflammation levels in atherosclerotic plaques	[59]
Multimodal imaging strategies							
PAI/SPECT/CT	Pd@Au-PEG-FA	~31 nm, nanosheet-like	providing PAI, SPECT, and CT signals, high targeting, low background	folic acid	FR on activated macrophages	imaging activated macrophages and vulnerable plaques	[60]
PAI/MRI/ultrasound	EWVDV-Fe-Ink-PFH NPs	~387.1 nm, spheric	providing PAI, MRI, and US signals, high targeting	EWVDV peptide	P-selectin on activated platelets	imaging thrombi	[61]
OCT/IR	IR-QD	~5 nm, spheric	providing OCT and PL signals	NA	NA	NA	[62]
XEL/MRI	XEL-NCs	~21.9 nm, spheric	providing XEL and MRI signals, background-free and turn-on properties	peptide	thrombin	monitor thrombosis progression	[63]

TPP$_{1880}$/LMWF$_{8775}$ CNPs, self-assembled complex nanoparticles with depolymerized low-molecular-weight fucoidan (LMWF$_{8775}$) and a thermolysin-hydrolyzed protamine peptide (TPP$_{1880}$); Ag$_2$S-AngII, AngII-functionalized Ag$_2$S nanodots; AngII, angiotensin II; AT1R, angiotensin receptor 1; TfR1, transferrin receptor 1; ^{64}Cu-CANF-comb, ^{64}Cu labeled, c-atrial natriuretic peptide conjugated polymeric (comb) nanoparticles; NPRC, clearance natriuretic peptide receptor; PBD-CD36 NPs, an anti-CD36 decorated semiconducting polymer NPs; Pd@Au-PEG-FA, folate-conjugated Pd@Au nanomaterials; XEL-NCs, X-ray luminescent lanthanide-doped scintillator nanocrystals.

field of the rapid detection of miRNAs related to CADs.[30–32,53,54] They synthesized a hemin-bridged metal-organic framework (MOF) as a functional interface to boost the payload and catalysis of G-quadruplex (G4) DNAzymes (Figure 1F).[32] Compared with previous smartphone-based counterparts, this new facile methodology showed both six orders of magnitude higher sensitivity and an ~50-fold longer duration for CL miRNA imaging.

Overall, nanomaterial-based biosensors provide precise, specific, simple, and rapid strategies to detect various biomarkers, which will greatly influence the diagnosis of CADs. However, the clinical transformation of nano-biosensors still requires extended work.

Nanotechnology-assisted molecular imaging for CAD diagnosis

In this section, we will demonstrate the critical function of nanotechnology in different imaging strategies and the information on CADs provided by nanomaterial-based molecular imaging, as summarized in Tables 2 and S2.

Magnetic resonance imaging. Magnetic resonance imaging (MRI), as a mainstream noninvasive imaging technique, is suitable for characterizing abnormal blood vessel walls with plaques and thrombi. Compared with positron emission tomography (PET) or computed tomography (CT), MRI does not employ ionizing radiation, unlike ultrasound and optical methods, which cannot provide deep tissue penetration. MRI also has advantages over PET because of its much higher spatial resolution (submillimeter).[64,65] Benefiting from this advantage, three-dimensional time of flight (3D TOF) and fast spin-echo (3D FSE) magnetic resonance angiography imaging were recently utilized to image carotid atherosclerotic plaques, and the lipid core volume, fibrous cap thickness, and hemorrhage volume were well determined.[66] In addition, with the help of stress calculations and tissue strength assessment based on multicontrast MRI and MRI-inflammation imaging, plaque rupture risk potential could be fully evaluated.[67] However, one of the drawbacks of MRI is the much lower sensitivity

of contrast agent detection compared with nuclear techniques. Hence, designing sensitive and specific probes for abundant accumulation at vessel lesions is critical for promoting the application of MRI in the diagnosis of CADs. Recently, MR-dedicated contrast agents, especially Gd-based and iron oxide nanoparticles, have been explored for the molecular imaging of atherosclerosis and thrombosis.[68–74] Due to their own characteristics, nanoparticles based on Gd or iron oxide show clear contrast effects in T_1/T_2-weighted MRI. Additionally, ultrasmall sizes at the nanolevel combined with ingenious surface modifications, including biocompatible coatings (polymers or cell membranes) and targeting elements (antibodies, peptides, or ligands), greatly increase the specific accumulation of MRI nanoprobes in ruptured or rupture-prone lesions and confer a longer circulation time.[75] Therefore, these targeted Gd-based and iron oxide nanoparticles have shown that MRI can be performed with sensitivity feasible for the diagnosis of atherosclerotic plaque formation, major components, and related diseases such as inflammation, paving the way for future clinical applications.

Recently, Zhang et al. designed highly sensitive magnetic iron oxide nanocubes (MIONs) to detect myocardial infarction (MI) via MRI (Figure 2A).[76] In experiments, the zwitterionic biodegradable copolymer poly(lactide) polycarboxybetaine (PLA-PCB, PP), accompanied by phosphatidylserine (PS), provided superior colloidal stability, long blood circulation, and a low T_2 signal for nanocubes to overcome the hydrophobic properties and insufficient delivery of MIONs as MRI contrast agents. PS can bind to PS receptors on the macrophage surface during early inflammation in MI. Similarly, engineered hybrid metal oxide-peptide amphiphile micelles (HMO-Ms) were constructed for potential use in MRI of thrombosis on atherosclerotic plaques.[77] The HMO consisted of inorganic, magnetic iron oxide cores with organic, fibrin-targeting peptide (CREKA) amphiphiles. These self-assembled, 20- to 30-nm spherical nanoparticles were found to be biocompatible with human aortic endothelial cells *in vitro* and to bind to human clots three to five times more efficiently than their nontargeted counterparts,
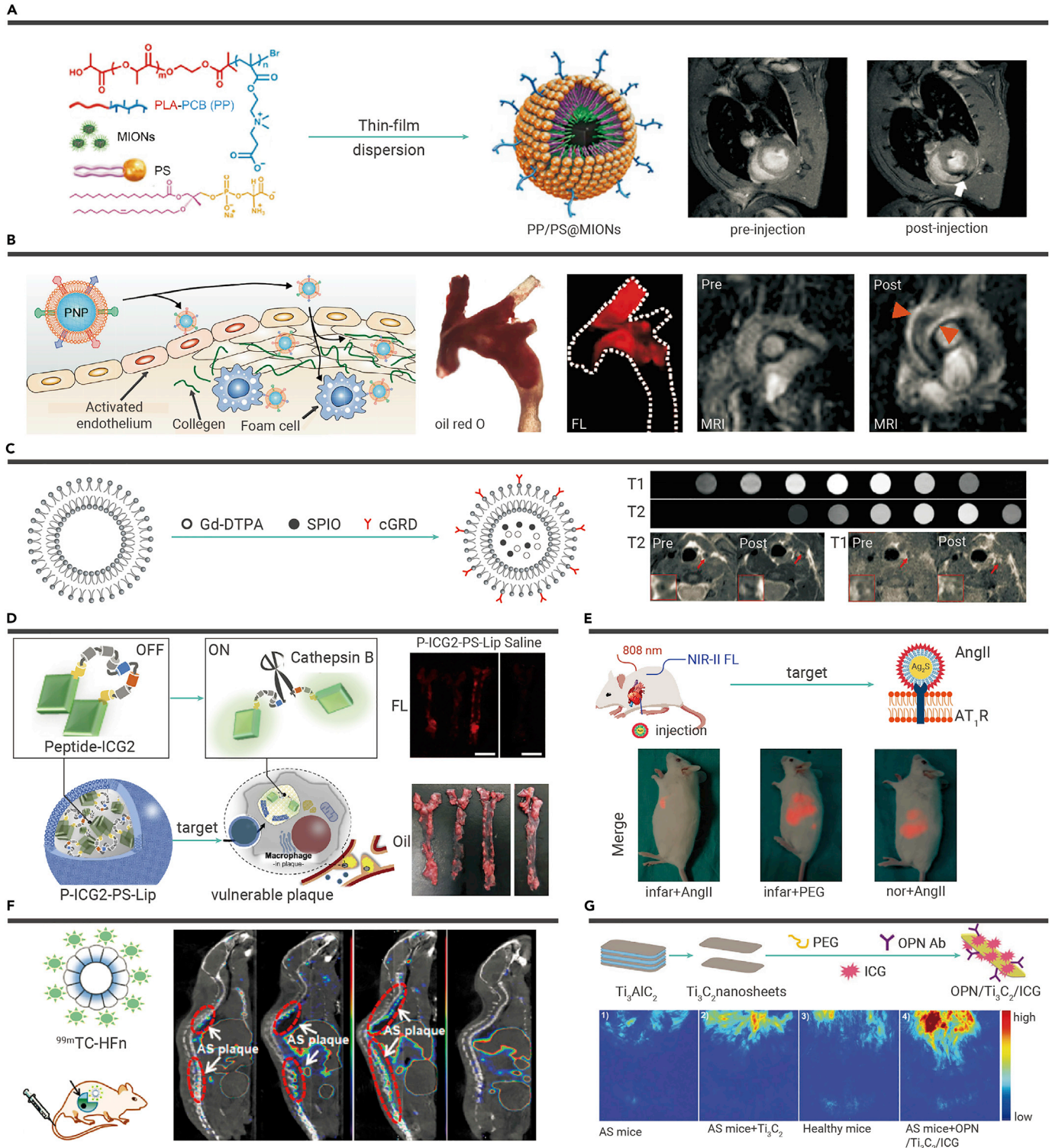
Figure 2. Various nanotechnology-based molecular imaging methods (A) PP/PS@MIONs used in MRI imaging of MI.[76] With external magnetic field-induced targeting and PS targeting, the PP/PS@MIONs nanosystem enhanced the accumulation in infarcted area, showing accurate MRI-based visualization of MI at an early stage. (This is an open access article distributed under the terms of the Creative Commons Attribution [CC BY-NC] license.) (B) Platelet membrane-coated nanoparticles for magnetic resonance imaging activated endothelium, collagen, and form cells in plaques.[79] Biomimetic PNPs could not only bind to advanced plaques but also probe the pre-atherosclerotic lesions (copyright American Chemical Society, 2018). (C) T_1/T_2 dual-mode MRI for detecting thrombus.[80] cRGD@MLP-Gd exhibits a T_2 contrast enhancement at 1 h after intravenous administration, followed by a visibly larger T_1 contrast enhancement at the thrombus site (copyright Royal Society of Chemistry, 2020). (D) "Off-on" nanoprobe P-ICG2-PS-Lip for optical imaging of macrophages in vulnerable plaques.[81] Note that the peptide-ICG2 was optically silent under normal conditions but activated in the presence of the lysosomal enzyme, cathepsin B. The NIRF fluorescent signal of P-ICG2-PS-Lip was successfully observed at the plaques on the artery walls (copyright Elsevier Ltd., 2020). (E) NIR-II nanoprobe used in optical imaging of MI.[56] With the analysis of time course experiments, the AngII-Ag$_2$S NDs could specifically accumulate at the ischemic myocardial tissues after intravenous injection within a few minutes, which opens a new avenue toward cost-effective, fast, and accurate in vivo imaging of the ischemic myocardium after AMI (copyright Wiley-VCH, 2020). (F) ^{99m}TC-HFn nanotracer for PET imaging of vulnerable plaques.[82] The specific uptake of ^{99m}Tc-HFn in plaques enabled quantitative measuring of the vulnerable and early active plaques as well as dynamic changes of inflammation during plaque progression (copyright American Chemical Society, 2018). (G) OPN/Ti$_3$C$_2$/ICG nanoprobe for accurate PAI of vulnerable plaques.[83] OPN/Ti3C2/ICG possessed enhanced PA performance and high specificity to foam cells in vulnerable atherosclerotic plaques (copyright Wiley-VCH, 2020).

offering potential for the early diagnosis of thrombosis in atherosclerosis. Zhou et al. explored profilin-1 antibody (PFN1)-loaded paramagnetic iron oxide nanoparticles in a complex with low-pH-sensitive cyclodextrin (PFN1-CD-MNPs) for the MRI of atherosclerosis.[78] Due to the specific binding of PFN1 to vascular smooth muscle cells (VSMCs), the accumulation of PFN1-CD-MNPs in atherosclerotic plaques was found via both near-infrared fluorescence (NIRF) *ex vivo* and MRI *in vivo*.

In addition to loading target-specific biomolecules on organic or inorganic nanoparticles, cell membrane coating and nanoassembly with biomolecules are also capable of effectively localizing atherosclerotic plaques.[55,79,84] Platelets are involved in different stages of atherosclerosis progression, such as endothelial inflammation and immune cell recruitment. Therefore, platelet membrane-coated nanoparticles (PNPs) incorporating lipid-chelated Gd were synthesized by Zhang's group.[79] Live MRI imaging showed that the biomimetic PNPs could not only bind to advanced plaques but also probe preatherosclerotic lesions (Figure 2B). Based on the same principle, self-assembled complex nanoparticles (CNPs) composed of polymerized low-molecular-weight fucoidan (LMWF8775) and a thermolysin-hydrolyzed protamine peptide (TPP1880) were successfully prepared for imaging activated or inflamed endothelial cells with P-selectin overexpression. Compared with free Gd-DTPA, CNPs loaded with Gd contrast agent showed better T_1 relaxivity and selectively accumulated in activated HUVECs with increased MRI intensity and reduced cytotoxicity.[55] Recently, the same principle was also applied to PP1 peptide-functionalized, glutathione-biomineralized gold/gadolinium-based nanoparticles (GSH-PP1-Au/Gd-NPs) synthesized by Li et al.[84] The PP1 peptides could specifically bind to class AI scavenger receptors (SR-AI) on foamy macrophages, and GSH molecules could endow the nanoparticles with superior stability, negligible cytotoxicity, and excellent biocompatibility. These novel nanoprobes integrated T_1 signal amplification, precise macrophage targeting, and systematic clearance capabilities for the noninvasive characterization of vulnerable plaques of early-stage atherosclerosis.

To achieve highly accurate CAD diagnosis, researchers have attempted to combine complementary information obtained from multiple imaging techniques.[85] However, differences in the depth of penetration and spatial/time resolution of various imaging devices may lead to difficulties and discrepancies when matching images, resulting in interpretation inaccuracies.[86] For this reason, the development of dual imaging strategies employing a single technique and instrumental system would provide significant advantages. Whittaker's group generated ultrasmall magnetic dual-contrast iron oxide nanoparticles (DCIONs) by a high-temperature coprecipitation method, which acted as efficient positive and negative dual-contrast agents for MRI.[87] After tagging with a single-chain antibody (scFv), DCIONs could specifically bind to GPIIb/IIIa receptors on activated platelets. In the presence of scFv-DCIONs, thrombi were highlighted in T_1-weighted imaging by a bright/positive signal and in T_2-weighted imaging by a dark/negative signal generated around their surface. The duality of T_1 and T_2 conferred MRI stronger contrast and a smaller r_2/r_1 ratio, which greatly increased the sensitivity and accuracy of diagnosis. Similarly, cyclic RGD-functionalized liposomes (cRGD@MLP-Gd) encapsulated with Gd-DTPA and SPIO were prepared by Li's group (Figure 2C).[80] In their experiment, the dynamic T_1/T_2 dual-mode property not only made cRGD@MLP-Gd actively bind to thrombi but also potentially enabled the monitoring of rupture-prone atherosclerotic lesions.

Optical imaging. Optical imaging technology has made great improvements in biomedical research. The prominent features of spatial resolution (micrometer-range), high sensitivity of (sub)cellular localization, lack of radiation, and cost effectiveness features make it attractive for the imaging atherosclerotic plaques and clots.[88–91] However, the poor penetration depth of light (from submillimeters to several centimeters) and undesirable overlap with autofluorescence in plaque tissues reduce the potential application of optical imaging platforms in the clinic. Fortunately, NIRF, with reduced tissue autofluorescence background and scattering and enhanced tissue penetration, presents an exciting method for the identification of atherosclerotic lesions at the molecular level.[92–94]

NIR-1 dyes, with emission peaks in the range of 700–900 nm, have higher signal-to-background ratios than visible probes.[95,96] Functional nanoparticles (such as polymeric nanoparticles, liposomes, and iron oxide nanoparticles) can serve as carriers to transport NIR-I dyes to plaque sites or can be designed as activated fluorescent "off-on" switches for NIRF imaging of atherosclerotic plaques or thrombi. Cy5.5-labeled hyaluronan nanoparticles (HA-NPs) were synthesized to investigate the endothelial barrier integrity and the enhanced permeability and retention (EPR) effect during atherosclerosis progression in Apoe−/− mice.[97]

The results showed that HA-NPs first entered the plaque via endothelial junctions, then distributed throughout the ECM and were eventually engulfed by plaque-associated macrophages. These features enabled HA-NPs to reflect the different stages of plaque progression during the treatment. Experiments with similar principles showed that a multivalent nucleic acid-scavenging nanoprobe (Dex-TO) synthesized through the conjugation of fluorochrome thiazole orange (TO) and polymer dextran carrier (40 kDa) was able to identify MI injury effectively with fluorescence reflectance imaging.[98] Activatable fluorescent "off-on" probes have already been designed in recent years for the targeted molecular imaging of plaques and thrombi, which could further reduce the background and increase the specificity of diagnosis. Ogawa et al. synthesized a fluorescent switch-on nanoprobe, peptide-ICG2 encapsulated in a phosphatidylserine liposome (P-ICG2-PS-Lip), for the specific imaging of macrophages in vulnerable plaques (Figure 2D).[81] Similarly, thrombin-activatable fluorescent peptide (TAP)-incorporated silica-coated gold nanoparticles (TAP-SiO$_2$@AuNPs) were developed for the direct imaging of thrombi.[99] The TAP-SiO$_2$@AuNPs showed a quenched NIRF signal under normal conditions due to the excellent quenching effect of SiO$_2$@AuNPs. In the presence of thrombin *in vitro*, a 30.31-fold higher NIRF intensity was rapidly recovered because of the thrombin-specific cleavage of TAP molecules on the SiO$_2$@AuNP surface. Additionally, TAP-SiO$_2$@AuNPs successfully accumulated in thrombi by size-dependent capture and clearly distinguished thrombotic lesions from peripheral tissues in NIRF/micro-CT imaging.

The emergence and development of new technologies have led to novel fluorescent nanoparticles emitting in the second NIR window (NIR-II, 1,000–1,700 nm), which allows NIRF imaging to visualize deep tissues with an unprecedented degree of clarity for diagnosis or surgical guidance.[100–103] Some novel biofunctionalized NIR-II nanoparticles, such as quantum dots (QDs),[56,104,105] single-walled carbon nanotubes (SWNTs),[106,107] and rare earth-based upconversion nanoparticles (UCNPs),[108–110] have been reported for the *in vivo* imaging of atherosclerosis or AMI, which will help to expedite the clinical transition of NIR imaging. Although differentiating vulnerable plaques from stable plaques remains challenging in the clinic, Gao et al. developed highly luminescent, macrophage-specific core@shell-structured NaGdF$_4$: Yb, Er@NaGdF$_4$ nanoprobes (UCNP-*anti*-OPN probe) to visualize vulnerable atherosclerotic plaques.[108] The core@shell structure maximized the contrast-enhancing performance, and the luminescence intensity of the core was well preserved after surface PEGylation through the ligand exchange process. In addition, surface PEGylation enabled the covalent conjugation of antibody-sensing osteopontin (OPN), which is a secreted biomarker associated with macrophages and foamy macrophages that can be used to identify vulnerable plaques. This UCNP-*anti*-OPN nanoprobe produced different optical signals between vulnerable and stable plaques by lowering shear stress and oscillatory shear stress, implying that the probe and imaging strategy were potentially useful for the precise diagnosis of atherosclerotic plaques. In a study of MI, Nuria Fernández et al. employed angiotensin II (AngII)-functionalized Ag$_2$S nanodots (AngII-Ag$_2$S NDs) for NIR-II *in vivo* imaging of ischemic myocardium after AMI (Figure 2E).[56] This method of fast and precise localization of ischemic tissues in the myocardium after AMI is needed by clinicians as the first step toward accurate and efficient therapy.

Nuclear scintigraphy. Among various imaging technologies, radionuclide-based molecular imaging has been widely exploited for the diagnosis of atherosclerosis due to its high sensitivity, quantification, functional detection, noninvasive nature, and well-established pathways for human translation.[111,112] With outstanding capacities, PET shows 2−3 times better spatial resolution than SPECT and allows the detection of picomolar concentrations of nuclide agents.[113] ^{18}F-fluorodeoxyglucose (^{18}F-FDG)-based PET, which can detect vascular inflammation and macrophage burden, has been proposed as the noninvasive gold standard for atherosclerotic plaque vulnerability identification.[114] However, its limited spatial resolution (~2 mm) and high myocardial metabolic uptake (resulting in a lack of specificity for atherosclerosis) have restricted the scope of the clinical application of ^{18}F-FDG PET. In particular, the small size of vascular plaques requires a higher accumulation of focal, targeted, and specific ^{18}F-FDG. Therefore, radiotracers that are more specific for inflammation and better suited for vascular lesion imaging are of intense interest for the sophisticated characterization of atherosclerosis.

To overcome these shortcomings of existing radiotracers, biofunctional nanoprobes labeled with radionuclides and targeting elements have been proposed. Liu's group constructed a poly(methyl methacrylate)-core/polyethylene glycol-shell amphiphilic comb-like nanoparticle conjugated with viral macrophage

inflammatory protein-II (vMIP-II).[115] After radiolabeling with ^{64}Cu, the biofunctional nanoparticles sensitively and specifically detected chemokine receptors in both mouse vascular injury models and atherosclerosis models. In the process of plaque formation, chemokine receptors are upregulated in macrophages.[116,117] Thus, the ^{64}Cu-vMIP-II-comb nanoprobe for PET imaging could be able to identify plaque progression.[115] Another successful example was the bioengineering of natural heavy-chain ferritin (HFn) nanocages radiolabeled with technetium 99m (^{99m}Tc-HFn) for the SPECT/CT imaging of vulnerable atherosclerotic plaques.[82] This focal ^{99m}Tc-HFn uptake *in vivo* was observed in atherosclerotic plaques with multiple high-risk features such as macrophage infiltration and active calcification and in early active ongoing lesions with intense macrophage infiltration (Figure 2F). This strategy was superior to the noninvasive gold standard ^{18}F-FDG and the promising calcification activity imaging agent ^{18}F-NaF due to its high sensitivity and specificity for the quantitative detection of early plaques. Notably, HFn nanocages exist naturally in humans and are composed of nontoxic globular proteins (8–12 nm) that do not activate inflammatory or immunological responses.[118]

Apart from targeting macrophages, foam cells (Figure 2G) in plaques, natriuretic peptides, and their natriuretic peptide receptors have been largely neglected as potential targets for the imaging or therapy of atherosclerosis.[119] Relevant research has demonstrated that the clearance receptor (NPRC) acts as a biomarker for atherosclerosis in both human coronary arteries and animal models.[120] Thanks to that foundation, Pamela K. Woodard et al. conjugated NPRC binding peptide and C-type atrial natriuretic factor (CANF) to produce well-defined comb nanoparticles (CANF-comb) for the PET imaging of atherosclerosis in a mouse apoE−/−model.[57] In that experiment, 25% ^{64}Cu-CANF-comb could efficiently bind to upregulated NPRC located on atherosclerotic plaques, exhibiting impressive sensitivity and targeting specificity during the progression of atherosclerotic plaques. Furthermore, the imaging ability and clinical transformation potential of ^{64}Cu-CANF-Comb nanoparticles were verified for the imaging of complex atheromatous plaques in a rabbit double injury-induced atherosclerosis model and *ex vivo* human CEA (carotid endarterectomy) specimens.[58]

Multimodal imaging strategies. Each single imaging modality possesses its own unique merits and intrinsic drawbacks. In clinical diagnosis, MRI shows excellent high spatial resolution but low sensitivity, and NIRF imaging is attractive due to its high sensitivity, low background, and low cost but has unsatisfactory tissue penetration depth. PET imaging provides brilliant sensitivity but involves ion radiation and has only low spatial resolution. Therefore, multimodality fusion is currently an important trend in imaging technology. The combination of multiple imaging modalities yields complementary diagnostic information and offers synergistic advantages over a single imaging modality,[70,121–126] resulting in more sensitive and accurate detection of CADs.

The first mentioned multimodal fusion is the nanoparticle-based PET/MRI dual-modal imaging method,[127–131] which displays excellent potential with high resolution from MRI and deep tissue penetration from PET. Accordingly, Keliher et al. described a modified polyglucose nanoparticle, ^{18}F-Macroflor, with high avidity for macrophages, which was enriched in cardiac and plaque macrophages to increase PET signals in infarcts or atherosclerotic plaques in mice or rabbits (Figure 3A).[127] These dual-modal imaging data might provide information on orthogonal biomarkers that reflect macrophage biology in the future. In addition to macrophages, myeloid cells also participate in a complex immune response in ischemic heart disease. Mulder's group reported an imaging approach based on myeloid cell-specific and multimodal nanotracers.[131] The nanotracers are derived from high-density lipoprotein with a perfluoro-crown ether payload (^{19}F-HDL) and labeled with zirconium-89 and fluorophores, which could allow MRI, PET, and optical imaging simultaneously (Figure 3B). This multimodality imaging approach will be a valuable addition to the immunology toolbox, enabling the dynamic study of complex myeloid cell behavior. Besides, the combination of MRI and optical imaging for dual-modal imaging could effectively relieve their respective drawbacks: the low sensitivity of MRI and the poor tissue penetration and spatial resolution of optical imaging (Document S2).[108,132–138]

A recently emerged biomedical imaging modality is photoacoustic imaging (PAI), which relies on the broadband acoustic waves generated from the interaction between nanosecond pulsed light and photoabsorbers in tissues.[139] PAI shares a common signal detection regimen with ultrasound imaging; therefore, it could combine high spatial resolution and traditional ultrasound depth penetration from selective optical absorption.[140] Different types of nanostructures

have been used to date for the PAI detection of CADs,[59] including CuS nanoparticles,[141] gold nanocages,[142] gold nanorods,[143] and graphene oxide.[144] Ge and his colleagues evaluated the feasibility of identifying vulnerable atherosclerotic plaques at the molecular level *in vivo* with noninvasive PAI nanoprobes.[83] They succeeded in fabricating osteopontin antibody (OPN Ab) and ICG (NIR fluorescence molecules) coassembled Ti_3C_2 nanosheets (OPN Ab/Ti_3C_2/ICG), which possessed enhanced PA performance and high specificity for foam cells in vulnerable atherosclerotic plaques (Figure 2G). Moreover, targeted nanomaterial-based PA imaging usually coordinates with other imaging techniques, such as MRI, optical imaging, ultrasound, SPECT, and CT, to achieve more accurate detection of atherosclerotic plaques and thrombosis progression.[60,61,139,145,146] For example, folate-conjugated 2D Pd@Au nanomaterials (Pd@Au-PEG-FA) were used to image folate receptor-positive activated macrophages, a prominent component in advanced vulnerable plaques.[60] After injection of Pd@Au-PEG-FA, strong signals were detected *in vivo* with SPECT, CT, and PA imaging in heavy atherosclerotic plaques, which were significantly higher than those of normal aortas (Figure 3C).

In addition to the above multimodal strategies, other nanomaterial-based combined schemes for the diagnosis of CADs, including optical coherence tomography (OCT)/infrared luminescence (IR) and X-ray-excited luminescence (XEL)/MRI, have also been reported.[62,63,147] For instance, IR-QDs emitting in the third infrared biological window (1.55−1.87 μm) were synthesized for intracoronary OCT/IR multimodal imaging.[62] Under single-line laser excitation at 1.3 μm, the IR-QDs could provide simultaneous backscattering contrast and efficient luminescence at 1.6 μm, which was confirmed in both aqueous suspensions and tissues by using IC-OCT clinical equipment. Recently, Yang's group developed thrombin-activatable scintillating nanoprobes for the background-free NIR-XEL imaging of thrombosis *in vivo*.[63] These nanoprobes were constructed from bright XEL-emitting lanthanide-doped scintillator nanocrystals (NCs) and thrombin cleavable dye-peptide conjugates (Figure 3D). Because the nanoprobes were also compatible with MRI, XEL/MR dual-modal imaging could be performed to confirm the imaging accuracy and realize the practical monitoring of thrombosis progression.

In summary, the construction of advanced nanoprobes for molecular imaging could offer versatile tools for target-specific visualization of the biological processes of atherogenesis: inflammatory infiltration, fibrotic response, formation of vulnerable plaques, and thrombosis. Although great progress has been made, the clinical translation of nanoprobe-based molecular imaging remains a challenge. First, the biocompatibility, pharmacokinetics, and safety of nanoprobes *in vivo* should be investigated clearly and deeply. Second, large-scale manufacturing of nanoprobes with controlled physicochemical properties is the foundation of promoting their application in the clinic. Third, research on the fates of nanoprobes in complex plaque microenvironments and biomarkers of the pathological changes in vulnerable plaques and thrombosis will continue to be the focus in the diagnosis and treatment of CADs in the future.

NANOTECHNOLOGY APPROACHES FOR THERAPY OF CADs

In this section, we will discuss nanotechnology approaches applied in the treatment of CADs based on nanomaterials' physicochemical property and surface modification. The nanotechnology's application in medical tissue engineering will be given in Document S3 and Figure S1.

Nanomaterials as smart carriers for drug delivery

Generally, smart nanocarriers encapsulate two parts: targeting moieties and therapeutic drugs. Therefore, targeting moieties, including peptides, antibodies, ligands, and cell membranes, could drive the nanoplatforms to the lesion microenvironment and target the components of interest (Figure 4). Owing to their high capacity and easy modification, diverse therapeutic drugs, such as chemicals, proteins, peptides, and nucleic acids, have previously been loaded into nanocarriers. Tables 3 and S3 summarize recently reported nanocarriers to deliver different drugs in detail.

Nanocarriers to deliver chemical drugs and plant monomers. Small-molecule drugs, such as statins, are widely prescribed medicines for lowering the risks of CAD.[158] However, systemic delivery of these chemical drugs can potentially induce dose-dependent adverse effects such as hepatoxicity and myopathy.[159] To overcome these issues, various nanocarriers have been synthesized to deliver small-molecule drugs targeting atherosclerotic plaques or thrombi. The specific
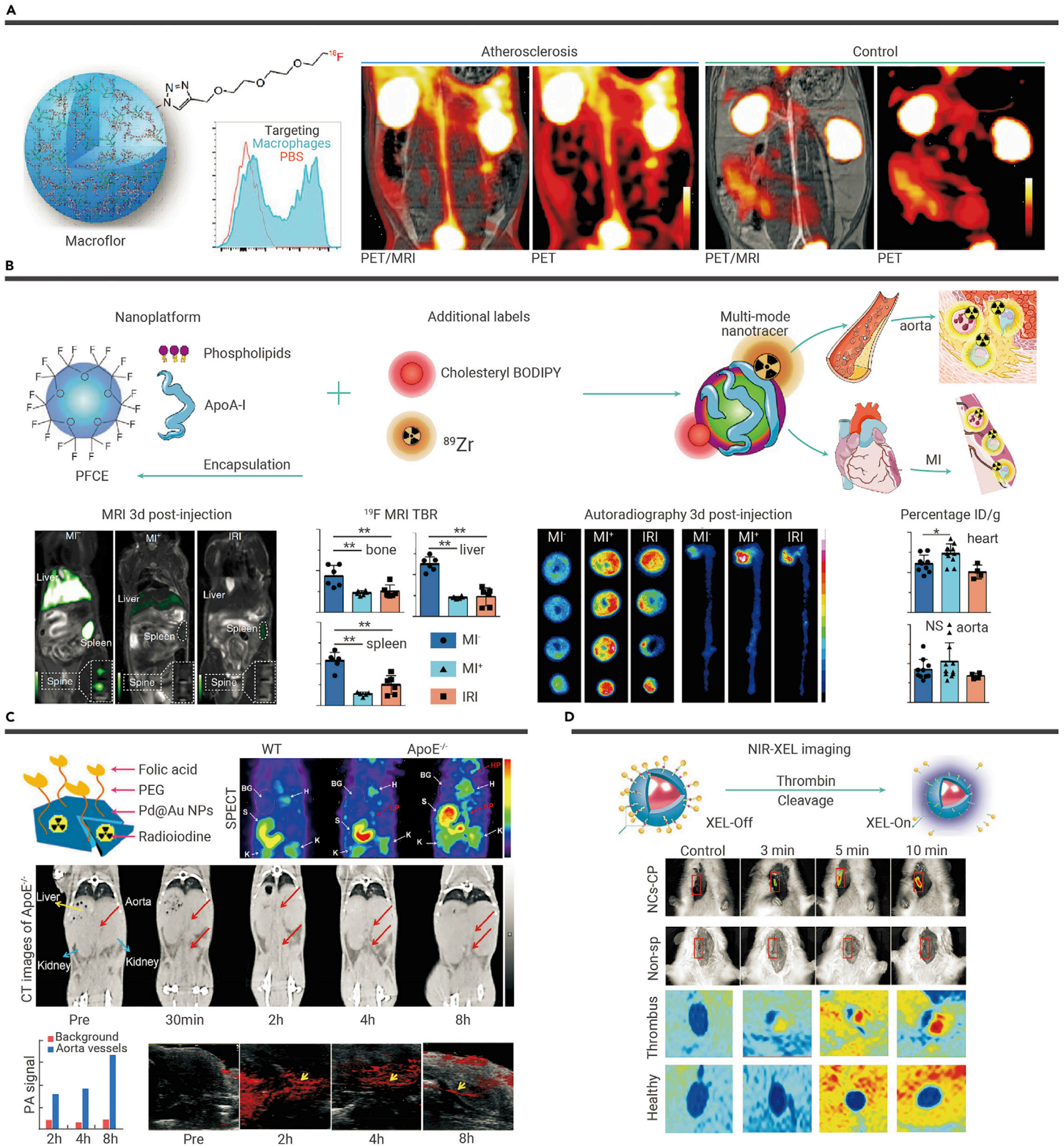
Review

Figure 3. Multimode imaging strategies for specific and accurate detection of atherosclerotic plaques and thrombi (A) Marcoflor nanotracer for PET/MRI to visualize athero-sclerosis.[127] In PET/MRI experiment, 18F-Macroflor PET imaging detected changes in macrophage population size, while molecular MRI reported on increasing or resolving inflammation (copyright Springer Nature, 2017). (B) [89]Zr-^{19}F-HDL nanotracer to monitor myeloid cell dynamic in atherosclerotic mice with myocardial infarction with PET/MRI.[131] With the [89]Zr label, the short-term dynamics and biodistribution of myeloid cells *in vivo* could be monitored at high levels of sensitivity by PET. Optical imaging could be used to study the associated cell subsets at a cellular level. The incorporated fluorine core allowed the nanotracer to quantify (by MRI) the myeloid cell dynamics up to 28 days post-injection, which remedied the physical decay of PET signals. With the integrative strengths of multimodal imaging, in atherosclerotic mice with myocardial infarction, the nanotracer displayed rapid myeloid cell egress from the spleen and bone marrow and their accumulation in atherosclerotic plaques and at the myocardial infarct site (*P < 0.05, **P < 0.01 and NS, no significance, two-sided Mann−Whitney *U*-test) (copyright Springer Nature, 2020). (C) Folate-conjugated 2D Pd@Au nanomaterials (Pd@Au-PEG-FA) for SPECT, CT, and PA imaging in heavy atherosclerotic plaques.[60] CT helped to restrict the pathological depiction more accurately. With synergistic effects from high sensitivity of SPECT and high resolution of CT, Pd@Au-PEG-FA produced strong PA signals that could provide structural imaging information of cardiac vasculature with high temporal and spatial precision (copyright Springer Nature, 2020). (D) Thrombin-activatable scintillating nanoprobes for NIR-XEL imaging of *in vivo* thrombosis.[63] Such nanoprobes showed XEL-off originally and enabled robust thrombin-activated turn-on XEL, which conferred XEL imaging background-free attribute and allowed it for detecting the early thrombosis on the basis of *in situ* elevated thrombin levels (copyright Wiley-VCH, 2021).
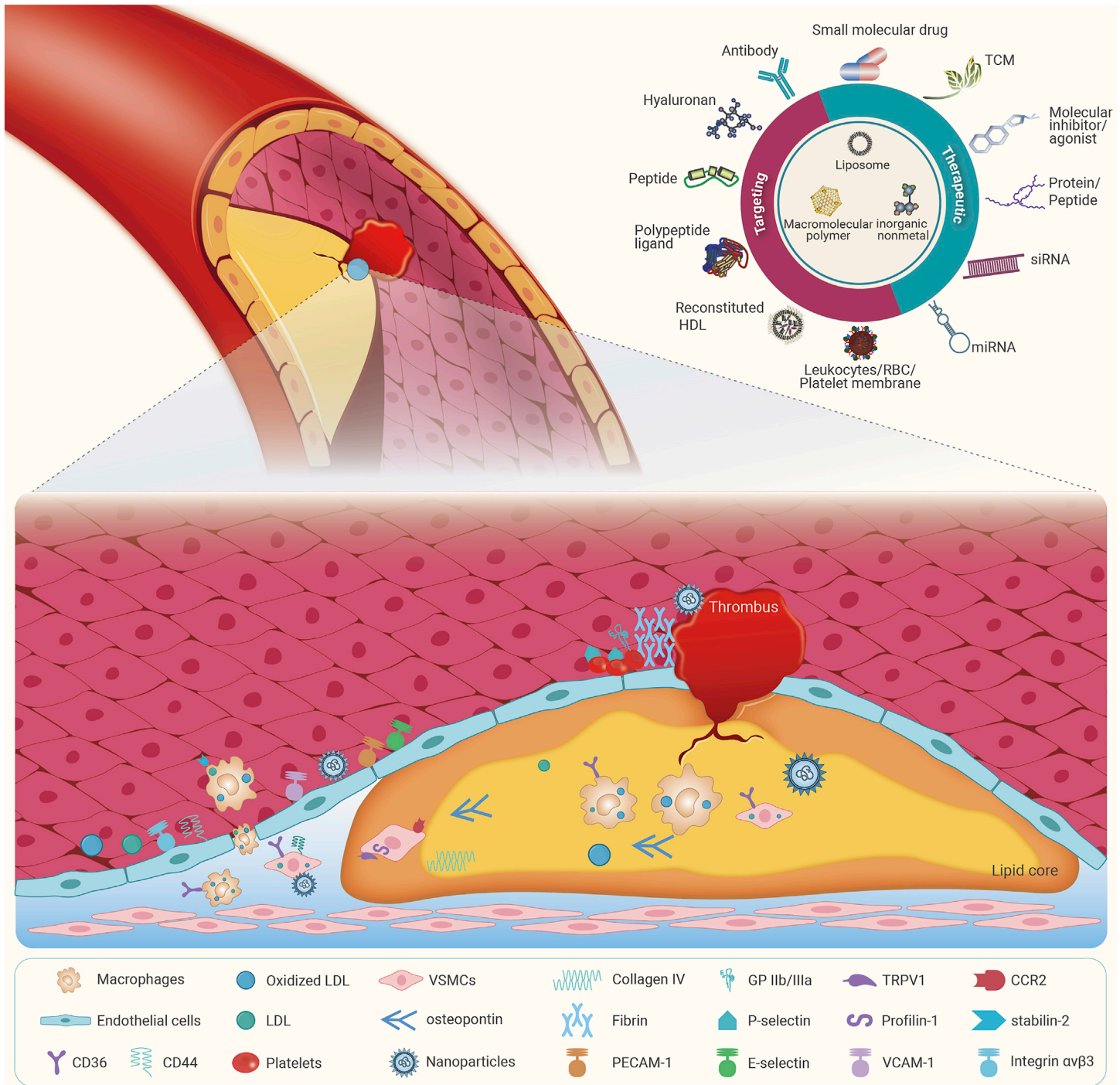
Figure 4. Multiple smart nanoplatforms targeting the lesion in the progression of atherosclerosis The surface modification of nanoplatforms via peptides, antibodies, ligands, and cell membranes could target different cells or components in the plaque to achieve precise delivery of chemicals, proteins, peptides, or nucleic acids and finally release these cargos to exert therapeutic effects.

accumulation of such drugs at lesions could increase their bioavailability and therapeutic effects.[128,148–150,160–163] Nanoparticles of the bioactive polymer hyaluronan (HA) with atorvastatin cores (HA-ATV-NPs) were synthesized to specifically bind with CD44, a cell surface receptor overexpressed on cells in atherosclerotic plaques.[164] The HA-ATV-NPs exhibited significantly higher anti-inflammatory effects on macrophages than ATV alone both *in vitro* and *in vivo*.[148] Simvastatin was loaded via a core/shell, cargo-switching nanoparticle (CSNP) composed of methyl-β-cyclodextrin (cyclodextrin, core) and phospholipids (shell) (Figure 5A).[161] Because cholesterol shows a higher affinity for cyclodextrin than for statins, systemically injected CSNPs could target atherosclerotic plaques, release statins, and scavenge cholesterol through cargo switching.[165] In an *in vivo* experiment, CSNP effectively prevented atherogenesis and caused the regression of established plaques.[161] In addition to targeted accumulation,

another major hurdle for the clinical application of nanodrugs is that most nanoparticles are taken up and removed by the reticuloendothelial system (RES) before reaching the target sites. To better escape RES clearance and achieve controlled payload release at plaque sites, Gao et al. developed macrophage membrane-coated reactive oxygen species (ROS)-responsive nanoparticles (MM-NPs) to encapsulate atorvastatin (MM-AT-NPs).[149] This biomimetic drug delivery system could not only prevent the clearance of NPs from the RES but also guide NPs to inflammatory tissues, enabling the specific release of atorvastatin after ROS activation. The inflammatory cytokine sequestration effect of the macrophage membrane further improved the therapeutic efficacy of MM-AT-NPs in atherosclerosis.[149] In addition to lipid-lowering drugs, anti-inflammatory medicines such as rapamycin and paclitaxel (PTX) can slow the progression of atherosclerosis through the inhibition of macrophage migration, smooth muscle

www.the-innovation.org

Table 3. Novel nanoplatforms for delivery of different drugs to the sites of CADs

	Loaded drug	Nanoplatforms	Disorders	Mechanism of action	Surface modifications	Model of use/ animal	Administration route	Ref
Statins	atorvastatin	HA-ATV-NP	atherosclerosis	suppression of inflammation	hyaluronan	in vitro; in vivo, Apoe−/− mice	intravenous injection	148
	atorvastatin	Oxi-COS/MM-AT-nps	atherosclerosis	suppression of inflammation	proteins derived from macrophages membrane	in vitro; in vivo, Apoe−/− mice	intravenous injection	149
Rapamycin	rapamycin	PFN1-CD-mnps	atherosclerosis	suppression of inflammation	profilin-1 antibody	in vitro; in vivo, Apoe−/− mice	intravenous injection	78
	rapamycin	liposome	atherosclerosis	suppression of inflammation	membrane protein from leukocytes	in vivo, Apoe−/− mice	retro-orbital injection	150
Traditional Chinese medicine	Sal B, PNS	RGD-S/P-lpns	AMI		RGD peptide ligand	in vivo, SD rats receiving experimental MI	intravenous injection	151
Small molecule agonists/ inhibitors	SMI 6877002	rHDL NPs	atherosclerosis	inhibition of monocyte recruitment; suppression of plaque inflammation	Apoa-I	in vitro; in vivo, Apoe−/− mice, cynomolgus monkeys	intravenous injection	152,153
Small molecule agonists/ inhibitors	SNO	SNO-HDL NPs	atherosclerosis		Apoa-I	in vitro; in vivo, Apoe−/− mice	intravenous injection	154
siRNA	siCamk2g	G0-C14 PLGA NPs	atherosclerosis	promotion of efferocytosis	S2P peptide (CRTLTVRKC)	in vitro; in vivo, Ldlr−/− mice	intravenous injection	155
miRNA	miR-145	PAM	atherosclerosis	promotion of the contractile VSMC phenotype	MCP1/CCL2	in vitro; in vivo, Apoe−/− mice	intravenous injection	156
miRNA switches	miRNA switches	mRNA-p5RHH nanoparticle	restenosis	specific inhibition of the VSMCs and inflammatory cells		in vitro; in vivo, C57BL6/J mice undergoing femoral artery wire injury	intravenous injection	157

HA-ATV-NP, hyaluronan-atorvastatin nanoparticle; Oxi-COS/MM-AT-nps, oxidation-sensitive chitosan oligosaccharide nanoparticles of amphiphilic/macrophage membrane-coated and atorvastatin-loaded nanoparticles; PFN1-CD-MNPs, low ph-sensitive cyclodextrin paramagnetic iron oxide nanoparticles conjugated with profilin-1 antibody; Sal B, salvianolic acid B; PNS, panax notoginsenoside; RGD-S/P-lpns, arginyl-glycyl-aspartic acid modified, Sal B and PNS co-loaded lipid-polymer hybrid nanoparticles; SMI 6877002, lipophilic small-molecule inhibitor of the CD40-TRAF6 interaction; rHDL NPs, reconstituted high-density lipoprotein nanoparticles; SNO, S-nitrosylated phospholipid, an NO donor compound; SNO-HDL NPs, S-nitrosylated phospholipid (1,2-dipalmitoyl-sn-glycero-3-phosphonitrosothioethanol) assembled with S-containing phospholipids and apolipoprotein A-I; G0-C14, a cationic lipid−like material; S2P peptide (CRTLTVRKC), a peptide recognizing the macrophage receptor stabilin-2; PS, phosphatidylserine; PAM, peptide amphiphile micelle; MCP1/CCL2, monocyte chemoattractant protein-1/C-C motif chemokine ligand 2; miRNA switches, modified mRNA encoding for the cyclin-dependent kinase inhibitor p27Kip1 that contains one complementary target sequence of miR126 at its 5′UTR.

cell proliferation, and neovascularization.[166–168] Good and workable solutions have been proposed to counteract the poor bioavailability and high toxicity of nanocarriers when taken by mouth.[169] One of those solutions was the synthesis of profilin-1 antibody-modified, pH-sensitive cyclodextrin/SPIONs to encapsulate rapamycin, which could effectively respond to the inflammation-produced acidic microenvironment and target VSMCs in atherosclerotic plaques.[78] Another was the conjugation of polypeptide C11 conjugated with polymer-lipid hybrid USPIO nanoparticles (UP-NP-C11) to load PTX to treat atherosclerotic lesions by macrophage internalization. In this experiment, the polymer-lipid hybrid component played an important role in achieving biocompatibility and stability in systemic circulation.[170]

To help nanocarriers escape the native immune system, different biomimetic design principles have emerged. Early in the progression of atherosclerosis, activated endothelium shows elevated levels of adhesion molecules and chemokines and induces the recruitment of leukocytes.[171] Therefore, leukocyte-based biomimetic nanoparticles named leukosomes can precisely target the inflamed areas in atherosclerotic lesions.[172] Recently, rapamycin was loaded in leukosome nanoplatforms. These biomimetic nanocarriers significantly inhibited the proliferation of macrophages and decreased the levels of proinflammatory cytokines, resulting in changes in the plaque morphology.[150] Another similar study indicated that macrophage membrane-coated nanoparticles with rapamycin cargos could also accumulate at activated endothelial cells, followed by effective suppression of macrophage phagocytosis and atherosclerosis progression in vivo (Figure 5B).[160] In terms of high affinity, platelets display inherent affinity for atherosclerotic plaques via different mechanisms, such as adhesion and aggregation.

Based on this, Song et al. developed PNPs encapsulating rapamycin, which could target atherosclerotic lesions and stabilize atherosclerotic plaques.[173] With higher biocompatibility, EPR, and longer half-life, the red blood cell (RBC) membrane has also been utilized to cloak nanoparticles.[174,175] Similarly, RBC membrane-coated PLGA could precisely deliver rapamycin to atherosclerotic plaques to attenuate the progression of atherosclerosis.[162] Compared with systemic delivery, local delivery of drugs with nanomaterial assistance would show better clinical effects, which could prevent restenosis after balloon angioplasty and reduce late adverse events of drug-eluting stents, such as late stent thrombosis.[163,176–178] Zhang's group designed a pH-sensitive and ROS-responsive β-cyclodextrin nanoplatform (Ox-bCD NPs) to deliver rapamycin to inflamed sites.[179,180] These dual-responsive NPs could passively target the injured vasculature and then inhibit the proliferation and migration of VSMCs by releasing rapamycin. The arterial restenosis rat model experiment showed that after intravenous injection, Ox-bCD NPs loaded with rapamycin could effectively attenuate neointimal hyperplasia. Since then, Zhu et al. designed bilayered nanoparticles (NPs) with the ability to sequentially release vascular endothelial growth factor (VEGF)-encoding plasmids from the outer layer and PTX from the core.[181] These bilayered nanomedicines were administered locally via balloon angioplasty to exhibit rapid endothelial regeneration and inhibition of restenosis.

As research on atherosclerosis advances, molecular inhibitors or agonists appear as new chemical drugs. It has been reported that monocytes/macrophages play an important role in the progression of atherosclerotic plaques, including the recruitment of monocytes to the vessel wall, the accumulation of macrophages,[182] phenotypic conversion,[183] and the secretion of inflammatory
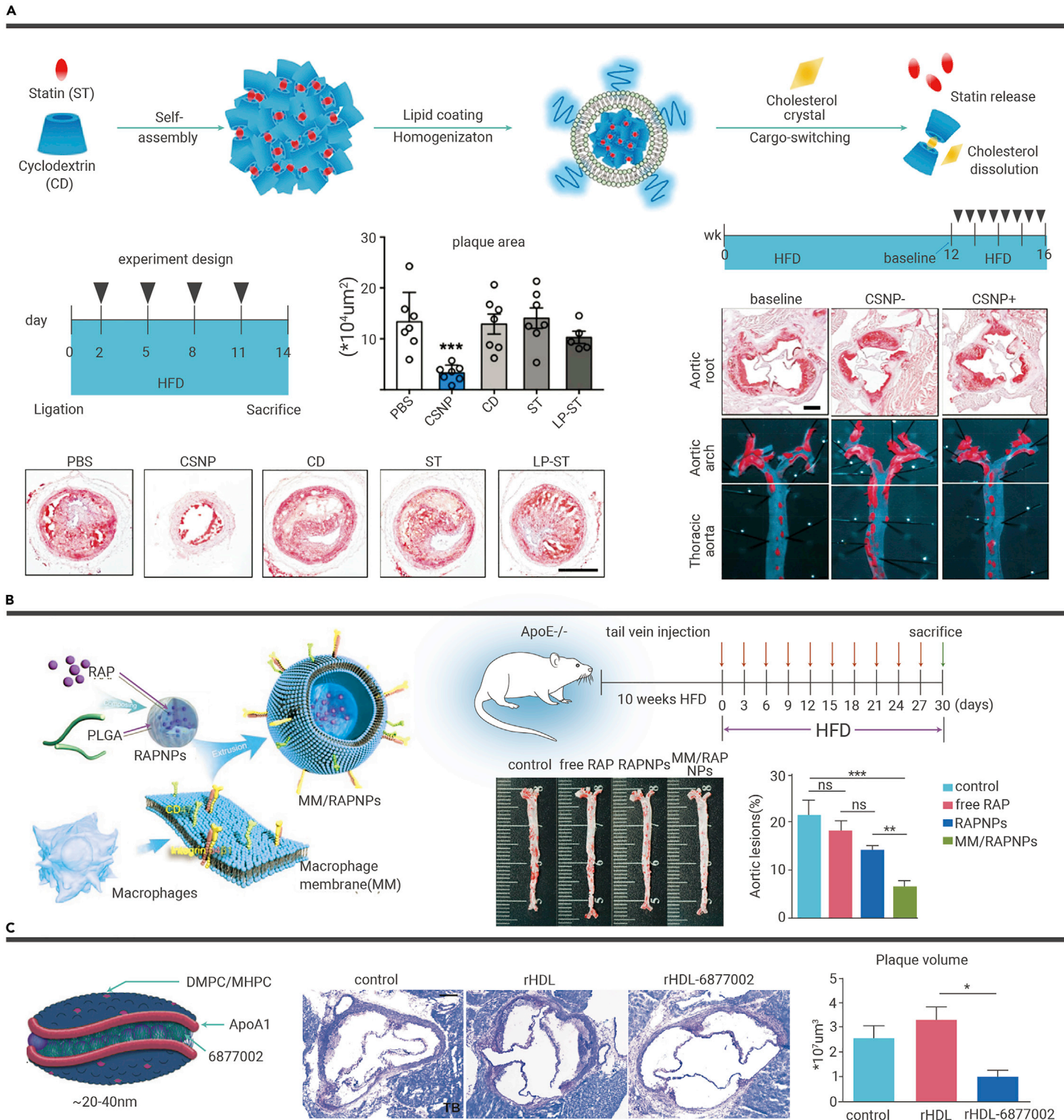
Figure 5. Nanocarriers to deliver chemical drugs (A) Cargo-switching CSNP to deliver statins, showing antiatherogenic effects and regression of atherosclerotic plaques. The scale bar indicates 200 μm (***P < 0.001, one-way ANOVA and Tukey's multiple comparison test) (copyright American Chemical Society, 2020).[161] (B) MM/RAPNP fabrication and its treatment for atherosclerosis in ApoE$^{-/-}$ mice.[160] MM/RAPNP could effectively suppress macrophage phagocytosis and atherosclerosis progression *in vivo* (**P < 0.01, ***P < 0.001 and ns, no significance) (This is an open access article distributed under the terms of the Creative Commons Attribution [CC BY-NC] license). (C) rHDL-6877002 for reducing plaque volumes and the number of macrophages.[153] Such CD4-TRAF6 blocking nanoimmunotherapy strategy could effectively inhibit monocyte recruitment and decrease plaque inflammation, as well as avoid the immune toxicity. Scale bar, 100 μm (*P < 0.05) (copyright Elsevier Ltd., 2018).

cytokines. Hence, it is promising to attenuate atherosclerosis progression via the efficient delivery of molecular inhibitors or agonists with nanocarriers to regulate targeting monocytes/macrophages. By virtue of the natural affinity to macrophages, novel reconstituted HDL nanoparticles were fabricated to deliver a small-molecule inhibitor (SMI 6877002) (Figure 5C).[152,153] The results showed that inhibitors could moderate CD40−CD40 ligand signaling in monocytes and

macrophages by blocking the interaction between CD40 and tumor necrosis factor receptor-associated factor 6 (TRAF6). Tang et al. established a combinatorial library of 17 HDL-mimicking hybrid nanoparticles and optimized their physicochemical properties to increase the targeting ability of a liver X receptor agonist (GW3965).[184] Among them, the nanoparticle with a POPC-dominant phospholipid composition, a long blood half-life, and a small size of 30 nm was the

most favorable and could abolish GW3965's liver toxicity while remaining effective on atherosclerotic plaque macrophages.[184] With collagen IV targeting ligand modification, these hybrid nanoparticles further improved the specific accumulation of GW3965 at atherosclerotic lesion sites.[185] Compared with the PBS group, mice administered Col IV-GW-NPs exhibited substantially reduced macrophage content (~30%) without increased hepatic lipid biosynthesis or hyperlipidemia. Tetsuya Matoba's group produced PLGA nanoparticles containing a chemical inhibitor of TLR4 intracellular domain-TAK-242 or pioglitazone (PPARc agonist).[186,187] The experimental data showed that both nanomedicines could effectively suppress inflammatory monocyte recruitment, promote the polarization of macrophages toward the M2 phenotype, and antagonize monocyte/macrophage-mediated acute inflammation after ischemia/reperfusion injury. SIRT1, as a molecule linked to the mTOR signaling pathway and autophagy, has the potential to prevent atherosclerosis.[188] To specifically deliver the Sirt1 activator SRT1720 to vulnerable atherosclerotic plaques, novel theragnostic nanomedicines (NMs) targeting OPN peptides (ICG/SRT@HSA-pept-NMs) were designed.[189] After intravenous injection into atherosclerotic mice, NMs were found to accumulate substantially at the lesions and achieve antiatherosclerotic effects by preventing VSMC phenotypic switching.

The controlled and sustained release of metabolic gas molecules (such as H_2S and NO) by nanocarrier-loaded substrates has therapeutic potential for the reversal of various cardiovascular pathophysiological processes.[154,190–192] A successful application of gas molecules was the use of mesoporous iron oxide nanoparticle-loaded diallyl trisulfide as an H_2S sustained-release system, with excellent attenuation of ischemia/reperfusion-induced myocardial injury in a mouse model.[192] According to the same theory, Jonathan et al. synthesized NO-delivering HDL-like particles (SNO-HDL NPs), which could reduce ischemia/reperfusion injury in vivo in a mouse kidney transplant model and atherosclerotic plaque burden in a mouse model of atherosclerosis.[154] Traditional Chinese medicine (TCM) has long been an effective complementary and alternative approach in China to the primary or secondary prevention of cardiovascular disease.[193] However, the physicochemical properties of TCMs, including low solubility, poor stability, and short half-life, limit their widespread clinical application. Fortunately, targeted delivery with nanocarriers such as inorganic metal nanoparticles and solid-lipid nanoparticles could effectively enhance the solubility and bioavailability of TCM, introducing new opportunities in CVD treatment (Document S4).[151,194–198]

Nanocarriers to deliver proteins and peptides. With further understanding of the pathological mechanisms and etiology of CVDs, coupled with rapid advances in materials engineering and biological techniques, many researchers took the opportunity to target atherosclerotic lesions with therapeutic proteins and peptides through nanoplatform-based drug delivery systems (Document S5).[199–205] For instance, with the assistance of poly(D-lactic acid) (PLA) and poly lactic-co-glycolic acid (PLGA) polymer NPs, interleukin 10 (IL-10) could be transported to atherosclerotic plaques via leaky endothelial junctions and bound to exposed collagen IV.[206] Moreover, the targeted NP polymer could provide controlled release of IL-10, resulting in increased cap size and decreased necrotic core size.

Nanocarriers to deliver nucleic acids. As an emerging therapeutic strategy, gene therapy has shown great potential in treating cardiovascular diseases. RNAi is a gene silencing modality that inhibits the expression of cell-specific genes or directly degrades their mRNA, showing promising performance in CVD intervention.[207]

Small interfering RNA (siRNA) can be utilized to mediate posttranscriptional regulation by binding to mRNA in a sequence-specific manner.[208] However, the clinical translation of siRNA therapeutics has been limited by several factors, including cytotoxicity, nuclease degradation and off-target effects, in recent years.[209] Benefiting from recent studies of the high targeting and stability of multifunctional nanocarriers in circulation, siRNA nanomedicines could rapidly penetrate disrupted plaque endothelial barriers and downregulate the expression of target genes locally, attenuating plaque inflammation in lesions.[210] The recruitment of arterial leukocytes triggered by adhesion molecules is one of the key points in the progression of atherosclerosis. To better inhibit recruitment, polymeric endothelial-avid nanoparticles encapsulating siRNAs were developed to simultaneously silence five essential adhesion molecules. With the protection of the above nanoparticles, the siRNAs could avoid degradation in serum and help prevent severe complications after acute MI.[211] In vivo, the low-molecular-weight ionizable polymer 7C1 was used to specifically deliver siRNA to the endo-

thelium to achieve efficient gene silencing in nonhuman primates, moving one step closer to the clinical translation of RNAi nanotherapy in atherosclerosis.[212] Recently, Shi's group first reported an siRNA NP platform targeting the plaque-destabilizing macrophage molecule Ca^{2+}/calmodulin-dependent protein kinase (CaMKII).[155] Compared with control siRNA NPs, atherosclerotic mice treated with siCamk2g NPs showed decreased CaMKII and increased MerTK expression in macrophages, improved phagocytosis of apoptotic cells (efferocytosis), decreased necrotic core area, and increased fibrous cap thickness. They designed a lipid-polymer delivery nanoplatform to address the limitations of systemic siRNA delivery (Figure 6A): cationic G0-C14 could effectively absorb the siRNA and enable its escape from late endosomes, whereas PLGA polymer was used to encapsulate the siRNA/C0-C14 complexes, protect the siRNA from serum nuclease degradation, and guarantee good biocompatibility. ATP-responsive nanocarriers to deliver siRNAs to lesions showed better selectivity and stability in circulation. Jiang et al. synthesized ATP-responsive low-molecular-weight polyethylenimine (LMW-PEI)-based supramolecular assembly to deliver SR-A siRNA via energy-dependent endocytosis to knock down SR-A mRNA and inhibit uptake of oxidized LDL.[213] After that, the same group fabricated a multifunctional core-shell nanoplatform with SR-A siRNA/catalase/ATP-responsive cationic carrier ternary polyplexes as the core and recombinant HDL modified with PS as the shell, which dynamically enhanced the targeting of macrophage CD36 in the plaques by establishing a positive feedback loop via the reciprocal regulation of SR-A and CD36.[214] After 4 weeks of repeated administration in vivo, positive feedback-enabled accumulation of the nanomedicines in the atherosclerotic plaques increased by 3.3-fold, resulting in reduced plaque areas by 65.8% and decreased macrophages by 57.3%.

MicroRNAs (miRNAs) are small noncoding RNAs that regulate gene expression posttranscriptionally by translational inhibition or degradation of target mRNAs by binding to 3′-untranslated regions (UTRs). Given that miRNAs are involved in multiple pathological processes, they might act as promising targets in the diagnosis and therapy of CVD progression.[216,217] However, miRNA-based therapies still face enormous challenges because of immune responses, degradation tendencies, off-target effects and toxicity, which could be solved through recent developments in nanotechnology-based drug delivery systems due to their high transfection efficacy, good resistance to nuclear enzymes, and flexible design for specific targeting.[218,219] Nguyen et al. developed 150- to 200-nm chitosan nanoparticles (chNPs) via the ionic gelation method with tripolyphosphate (TPP) as a cross-linker.[215] These chNPs were utilized to deliver miR-33 mimics to macrophages and downregulate the expression of its target gene ABCA1 both in vitro and in vivo, leading to decreased cholesterol efflux to apoA1 and reverse cholesterol transport (RCT). In contrast, when efflux-promoting miRNAs were delivered via chNPs, ABCA1 expression and cholesterol efflux into the RCT pathway were improved. This research indicated that miRNAs could be efficiently delivered to macrophages via nanoparticles to regulate ABCA1 expression and cholesterol efflux (Figure 6B). Furthermore, to make full use of cell surface nano-engineered technology and the advantages of graphene quantum dots (GQDs), such as miniature size, biocompatibility, and low cytotoxicity, Zhu's group developed a monocyte-C18PGQDs-miR223 nanoplatform.[220] In this experiment, disulfide bond-linked GQDs-miRNA223 were grafted onto the monocyte membrane through C18-peptide (C18P) with a hydrophobic end. After entering the interior of the atherosclerotic plaques, GQDs-miRNA223 were taken up by macrophages and achieved disulfide linkage cleavage in the lysosome. The released miRNA223 cargos ultimately translocated to the nucleus, resulting in significant degradation of target mRNA and relieving plaque burden. Similarly, Deborah et al. synthesized miR-145 micelles targeting C-C chemokine receptor-2 (CCR2), which is highly expressed on VSMCs. Compared with free miR-145 or PBS, the miR-145 micelles effectively mitigated atherosclerosis development by inhibiting plaque-propagating cell types derived from VSMCs.[156] This experiment indicated that miR-145 micelles prevented lesion growth by 49% and 35% in early-stage and mid-stage atherosclerosis, respectively.

Anti-miRNA or miRNA switches can also be transported to lesions by nanocarriers. Biofunctional polymer-lipid hybrid HDL-mimicking nanoparticles (HNPs) surface modified with Apo A1 were designed to load anti-miR155, which showed antioxidative ability and mediated cholesterol efflux.[221] Some studies have shown that synthetic mRNA can be posttranscriptionally regulated by miRNAs if miRNA complementary sequences are inserted into the 5′ or 3′ UTR.[222] These miRNA switches would allow the specific inhibition of the VSMCs and inflammatory cells that drive restenosis while sparing the injured endothelium. Lockhart
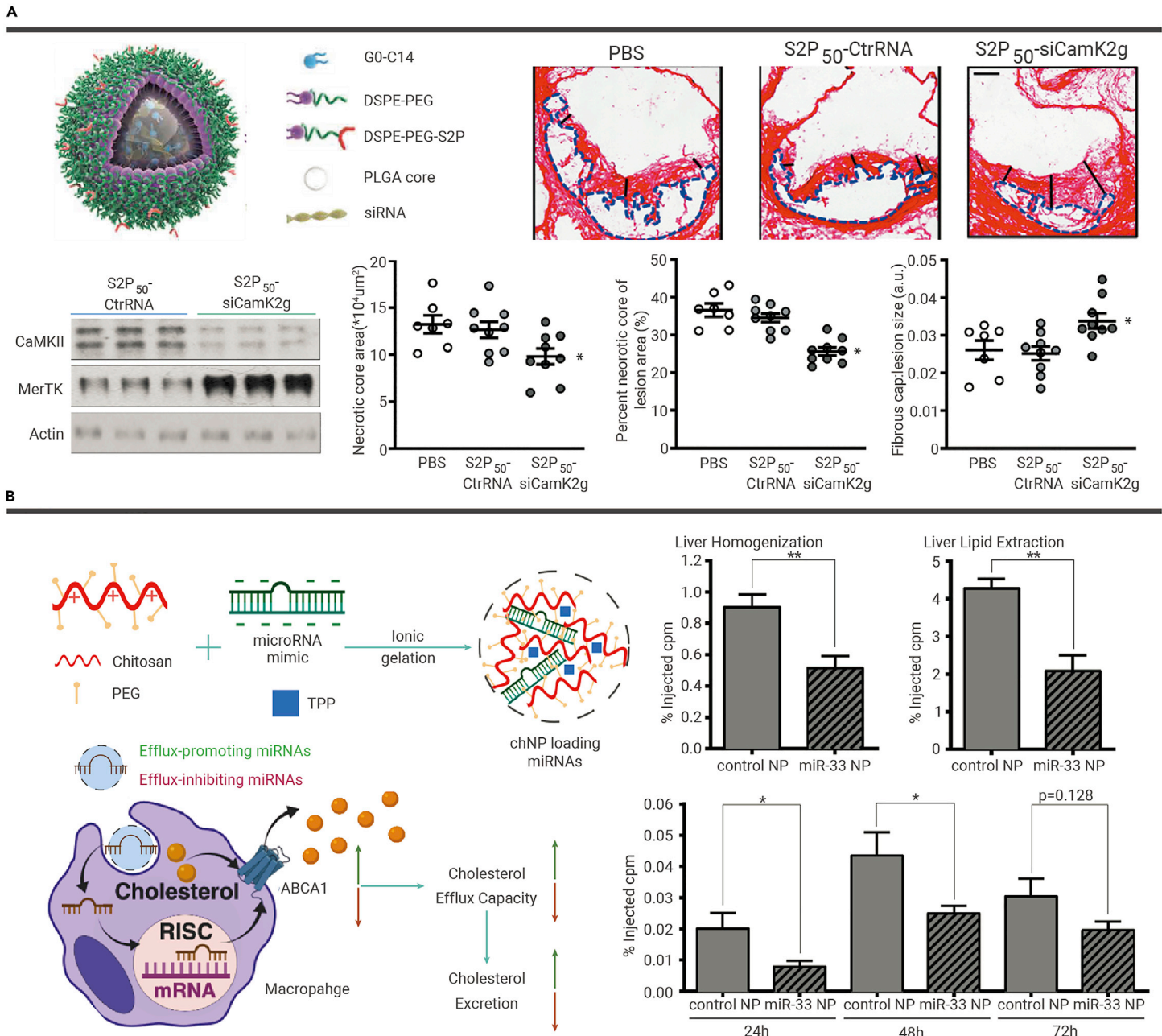
Figure 6. Nanocarriers for delivering therapeutic nucleic acids (A) Fabrication and silencing efficacy of S2P50-siCamk2g NPs. The lipid-PEG surface was used to stabilize the NPs, achieve an increased circulating lifetime, and avoid rapid clearance. Besides, the plaque macrophage-targeting peptide (S2P) was incorporated on the lipid-PEG layer, which further increases the specificity of targeting; treatment of WD-fed Ldlr−/− mice with S2P50-siCamk2g-loaded NPs lowers plaque necrosis and increases lesional efferocytosis. The scale bar indicates 200 μm (*P < 0.05, one-way ANOVA) (copyright American Association for the Advancement of Science, 2020).[155] (B) Schematic illustration of miRNA mimic-loaded chitosan nanoparticles prepared using the ionic gelation method; *in vivo* treatment with chitosan nanoparticles containing miR-33 inhibits RCT.[215] The injection of miR-33 NP resulted in the reduction of cholesterol efflux to apoA1 and reverse cholesterol transport (RCT) (*P < 0.05, **P < 0.01, Student's *t* test)(copyright American Chemical Society, 2019).

et al. synthesized p5RHH nanoparticles loaded with the cyclin-dependent kinase inhibitor p27Kip1 miRNA switch containing the complementary target sequence of miR-126 at its 5′ UTR.[157] This cell-selective nanotherapy significantly reduced neointima formation after wire injury and allowed reendothelialization *in vivo*, exhibiting potential capacity for treating neointimal hyperplasia, atherosclerosis, and restenosis.

Nanomaterials themselves act as therapeutic drugs

Ingeniously designed nanomaterials serve as vehicles for the targeted delivery of different therapeutics to atherosclerotic plaques and thrombi in many studies. Recent evidence has indicated that nanomaterials with intrinsic antioxidative and anti-inflammatory activities are promising next-generation therapies for the treatment of atherosclerosis, given the critical role of ROS in the pathogenesis of atherosclerosis and other inflammatory diseases. Hu's group cova-

lently conjugated the superoxide dismutase mimetic agent Tempol and the hydrogen peroxide-eliminating compound phenylboronic acid pinacol ester onto a cyclic polysaccharide β-cyclodextrin (TPCD), which was easily assembled into TPCD NPs and worked as a broad-spectrum ROS-eliminating nanomaterial.[223] Related research showed that TPCD NPs significantly attenuated ROS-induced inflammation and cell apoptosis in macrophages by eliminating overproduced intracellular ROS and effectively inhibited foam cell formation in macrophages and VSMCs by decreasing the internalization of oxidized LDL (Figure 7A). Antioxidant nanopolymers could also be used in antithrombotic therapy as a supplement to traditional thrombolytic agents due to fibrin aggregation and the elevated H₂O₂ level in thrombi. A fibrin-targeted imaging and antithrombotic nanomedicine (FTIAN) was constructed from NIR fluorescent dye-linked boronate antioxidant polymers and fibrin-targeting lipopeptides. This FTIAN could precisely image thrombi and inhibit thrombus formation by
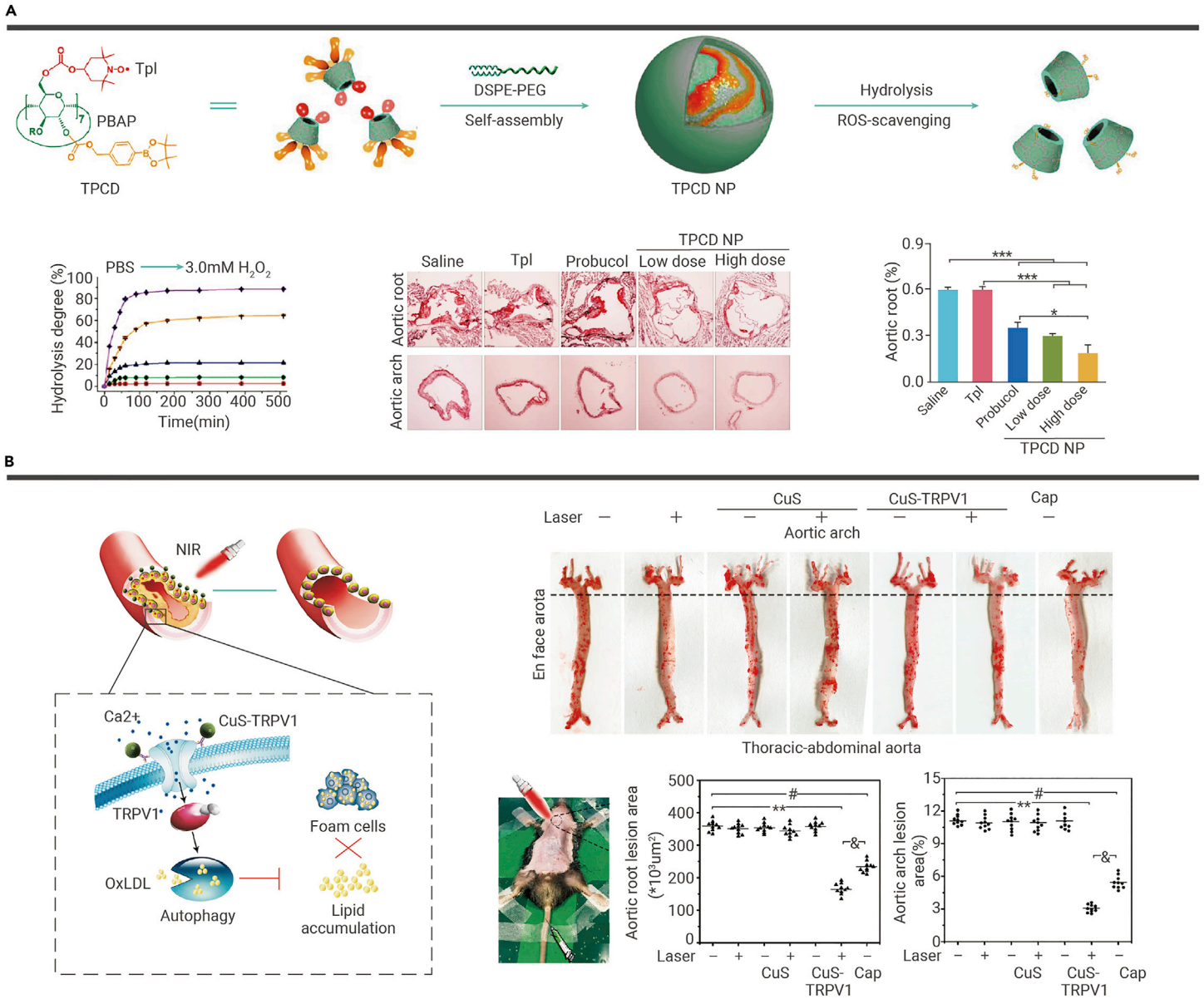
Figure 7. Nanomaterial themselves act as therapeutic drugs (A) Engineering of a broad-spectrum ROS-scavenging TPCD nanoparticle for targeted therapy of atherosclerosis.[223] After intravenous administration, TPCD NPs accumulated in atherosclerotic lesions in ApoE−/− mice by passive targeting, significantly inhibited the development of atherosclerosis, as well as stabilized advanced plaques. Scale bar, 200 μm (*P < 0.05, ***P < 0.001) (copyright American Chemical Society, 2018). (B) CuS-TRPV1 switch for photothermal activation of TRPV1 signaling to reduce atherosclerotic lesions.[141] With the photothermal property of CuS NPs, the TRPV1 channels opened and triggered calcium ions (Ca^{2+}) influx after NIR irradiation, leading to autophagy activation, cholesterol efflux, and impede foam cell formation (**P < 0.01 for CuS-TRPV1 + Laser vs. PBS, #P < 0.05 for Cap vs. PBS, &P < 0.05 for CuS-TRPV1 + Laser vs. Cap, Student's t test) (copyright Springer Nature, 2018).

scavenging H_2O_2.[146] In addition to the above polymer nanomaterials, metal-based inorganic nanomaterials also exhibit antioxidant properties and show promise for attenuating atherosclerosis progression. Optimal Se intake has been confirmed to prevent atherosclerosis due to its function of maintaining redox homeostasis and depressing oxidative stress.[224] However, the intricate Se species and the narrow safety window for Se intake limit the clinical utilization of Se supplementation.[225] To address the above problems, selenium nanoparticles (SeNPs) were developed, which showed high biological activity and bioavailability, low toxicity, and controlled release.[226,227] In vivo results indicated that SeNPs significantly reduced the lipid peroxidation level and simultaneously increased the NO level and the activities of glutathione peroxidase (GPx), superoxide dismutase (SOD), and catalase in the serum and liver.[228] Another example is the finding that nanosilver has been an innate antiplatelet property. Nanosilver can effectively prevent integrin-mediated platelet responses by accumulating within platelet granules and reducing interplatelet proximity.[229] Accordingly, gold (Au) and silver-gold alloy (Ag-Au) nanoparticles were green-synthesized as anticoagulant and thrombolytic agents by Ojo et al.[230]

Nanomaterial-assisted photodynamic therapy (PDT) and photothermal therapy (PTT) have emerged as promising therapeutic strategies for atherosclerosis and its related diseases. PDT has three key components: a photosensitizer, light, and molecular oxygen. To address the notable drawback of the shallow penetration of the traditional photosensitizer chlorin e6 (Ce6), upconversion nanoparticles composed of photosensitizer Ce6 and silica nanoparticles (UCNP-Ce6) were developed with enhanced penetration depth. The novel UCNP-Ce6 also exhibited high hydrophilicity, good biocompatibility, and favorable optical properties. Experimental results demonstrated that UCNP-Ce6-mediated PDT promoted cholesterol efflux by activating the autophagic process, which occurs in part through the ROS/PI3K/Akt/mTOR signaling pathway via ROS generation.[231] PTT is a minimally invasive, local treatment modality with minimal toxicity. It depends mainly on triggering a photosensitizer by electromagnetic radiation, such as radio frequency, NIR, or visible light, to convert this energy into heat. The temperature increase via PTT kills the cells in lesions. Copper sulfide NPs conjugated with transient receptor potential vanilloid subfamily 1 (TRPV1) monoclonal antibody (CuS-TRPV1) were designed and worked as a photothermal switch for

specific binding to TRPV1 on the surface of VSMCs (Figure 7B). Because of the photothermal property of CuS NPs, TRPV1 channels opened and triggered calcium ion (Ca^{2+}) influx after NIR irradiation, leading to autophagy activation and cholesterol efflux and impeding foam cell formation.[141] Furthermore, the research results indicated that CuS-TRPV1 reduced lipid storage and plaque formation *in vivo* with no obvious long-term toxicity, which suggested that CuS-TRPV1 has potential as a therapeutic tool to locally and temporally attenuate atherosclerosis.[141] Nanomaterial-mediated PTT for macrophage ablation has also shown promise in treating atherosclerosis.[232,233] Accordingly, semiconductor nanomaterial MoO_2 nanoclusters were synthesized and used for the first time in PTT for inflammatory macrophage (Mφ)-mediated atherosclerosis.[234] After optimizing the amount of nanomedicine and the treatment time, MoO_2-mediated PTT exerted the maximum ablation effect on Mφ and minimal damage to endothelial cells without requiring additional target moieties. In animal models, MoO_2-based PTT also showed an excellent therapeutic effect on atherosclerosis by eliminating Mφ with no significant side effects. Recently, to improve biosafety and ameliorate the thrombolytic effect, Yang's group explored dual-modal photothermal/photodynamic (PTT/PDT) thrombolysis.[235] They first fabricated RGD-modified mesoporous carbon nanospheres with porphyrin-like metal centers (RGD-PMCS), which could initiate site-specific thrombolysis by hyperthermia and ROS under NIR laser irradiation. Compared with single photothermal thrombolysis, RGD-PMCS-based dual-modal PTT/PDT thrombolysis could greatly increase the efficiency of thrombus breaking (87.9%) and prevent re-embolization into tiny fragments. This research demonstrated that dual-modal PTT/PDT provides a rapid, safe, and effective method for thrombolysis. Besides, nanomaterial-assisted high-intensity focused ultrasound or low-intensity focused ultrasound recently has been applied in novel thrombolytic strategy (Document S6).[236–238]

CONCLUSIONS AND PERSPECTIVES

Nanomaterials have been involved in the development of more precise biosensors to detect CAD biomarkers because of their size, increased diagnostic sensitivity, and shortened diagnostic time. In the future, nano-biosensors may be useful in portable devices applied in hospitals, households, ambulances, or chest pain centers. Second, compared with traditional imaging agents, nanomaterial-based molecular probes can specifically accumulate at atherosclerotic lesions through modification with different target moieties on the surface of nanoplatforms. Such purposive aggregations coupled with the high loading capacity or photoelectromagnetic properties of nanomaterials as well as multimodal imaging techniques will further improve the sensitivity and accuracy of imaging diagnosis in CADs. Beyond high-resolution imaging, nanotechnology has also taken an active part in the therapy of CADs (especially vulnerable plaques and thrombi) by different strategies, such as the repair of injured endothelium, anti-inflammation, antioxidation, and blockage of platelet recruitment.[239,240] In most cases, nanomaterials have served as multifunctional vehicles to deliver various therapeutic drugs, including chemicals, proteins, peptides, and nucleic acids. These nanocarriers not only have brilliant specificity endowed by target moieties but also increase drug bioavailability and protect the drugs from enzymolysis and clearance in the circulation. Moreover, the natural ROS scavenging and photodynamic or photothermal properties of nanomaterials still provide direct therapeutic strategies for CADs and intravascular implants.

Despite all this, nanotechnology has a long way to go from translational medicine to clinical application. (1) In clinical diagnosis, novel biomarkers must be screened for nanomaterial-based biosensors and molecular imaging approaches to estimate atherosclerosis progression. (2) In terms of treatment strategy, the biocompatibility, pharmacokinetics, and safety of nanomaterials *in vivo* should be carefully evaluated in both small (such as mice and rabbits) and large animal models (such as pigs and nonhuman primates) to obtain approval for clinical trials.[241] The fates of nanomedicines in complex plaque microenvironments and the interactions between nanomedicines and various components also need great attention. (3) Last but not least, the large-scale manufacturing of nanomedicines with controlled and stable physicochemical properties should be the key to the whole industrial operation due to the basic position of nanomedicines in clinical application.

REFERENCES

1. Benjamin, E.J., Muntner, P., Alonso, A., et al. (2019). Heart disease and stroke statistics-2019 update: a report from the American Heart Association. Circulation **139**, e56–e528.
2. Celermajer, D.S., Chow, C.K., Marijon, E., et al. (2012). Cardiovascular disease in the developing world: prevalences, patterns, and the potential of early disease detection. J. Am. Coll. Cardiol. **60**, 1207–1216.
3. World Health Organization. (2021). Cardiovascular Diseases (CVDs) (Geneva: World Health Organization).
4. Virani, S.S., Alonso, A., Aparicio, H.J., et al. (2021). Heart disease and stroke statistics-2021 update. Circulation **143**, e254–e743.
5. Linde, J.J., Kelbæk, H., Hansen, T.F., et al. (2020). Coronary CT angiography in patients with non-ST-segment elevation acute coronary syndrome. J. Am. Coll. Cardiol. **75**, 453–463.
6. Kyu, H.H., Abate, D., Abate, K.H., et al. (2018). Global, regional, and national disability-adjusted life-years (DALYs) for 359 diseases and injuries and healthy life expectancy (HALE) for 195 countries and territories, 1990-2017: a systematic analysis for the global burden of disease study 2017. Lancet **392**, 1859–1922.
7. Arbab-Zadeh, A., and Fuster, V. (2019). From detecting the vulnerable plaque to managing the vulnerable patient: JACC state-of-the-art review. J. Am. Coll. Cardiol. **74**, 1582–1593.
8. Daghem, M., Bing, R., Fayad, Z.A., et al. (2020). Noninvasive imaging to assess atherosclerotic plaque composition and disease activity: coronary and carotid applications. JACC Cardiovasc. Imag. **13**, 1055–1068.
9. Anderson, J., Adams, C., Antman, E., et al. (2013). 2012 ACCF/AHA focused update incorporated into the ACCF/AHA 2007 guidelines for the management of patients with unstable angina/non-ST-elevation myocardial infarction: a report of the American College of Cardiology Foundation/American Heart Association task force on practice guidelines. Circulation **127**, e663–828.
10. Levine, G.N., Bates, E.R., Blankenship, J.C., et al. (2011). 2011 ACCF/AHA/SCAI guideline for percutaneous coronary intervention: a report of the American College of Cardiology Foundation/American Heart Association task force on practice guidelines and the society for cardiovascular angiography and interventions. Circulation **124**, e574–651.
11. Ziaeian, B., and Fonarow, G.C. (2016). Epidemiology and aetiology of heart failure. Nat. Rev. Cardiol. **13**, 368–378.
12. Meng, H., Leong, W., Leong, K.W., et al. (2018). Walking the line: the fate of nanomaterials at biological barriers. Biomaterials **174**, 41–53.
13. Schulte, C., Barwari, T., Joshi, A., et al. (2019). Comparative analysis of circulating noncoding RNAs versus protein biomarkers in the detection of myocardial injury. Circ. Res. **125**, 328–340.
14. Yeh, H.W., and Ai, H.W. (2019). Development and applications of bioluminescent and chemiluminescent reporters and biosensors. Annu. Rev. Anal. Chem. (Palo Alto Calif.) **12**, 129–150.
15. Zanato, N., Talamini, L., Zapp, E., et al. (2017). Label-free electrochemical immunosensor for cardiac troponin T based on exfoliated graphite nanoplatelets decorated with gold nanoparticles. Electroanalysis **29**, 1820–1827.
16. Zhang, T., Ma, N., Ali, A., et al. (2018). Electrochemical ultrasensitive detection of cardiac troponin I using covalent organic frameworks for signal amplification. Biosens. Bioelectron. **119**, 176–181.
17. Yi, T.-Q., Gong, W., Lei, Y.-M., et al. (2018). New signal probe integrated with ABEI as ECL luminophore and Ag nanoparticles decorated CoS nanoflowers as bis-co-reaction accelerator to develop a ultrasensitive cTnT immunosensor. J. Electrochem. Soc. **165**, B686–B693.
18. Ye, J., Zhu, L., Yan, M., et al. (2019). Dual-wavelength ratiometric electrochemiluminescence immunosensor for cardiac troponin I Detection. Anal. Chem. **91**, 1524–1531.
19. Sun, D., Luo, Z., Lu, J., et al. (2019). Electrochemical dual-aptamer-based biosensor for nonenzymatic detection of cardiac troponin I by nanohybrid electrocatalysts labeling combined with DNA nanotetrahedron structure. Biosens. Bioelectron. **134**, 49–56.
20. Sun, D., Lin, X., Lu, J., et al. (2019). DNA nanotetrahedron-assisted electrochemical aptasensor for cardiac troponin I detection based on the co-catalysis of hybrid nanozyme, natural enzyme and artificial DNAzyme. Biosens. Bioelectron. **142**, 111578.
21. Zhang, J., Lakshmipriya, T., and Gopinath, S.C.B. (2020). Electroanalysis on an interdigitated electrode for high-affinity cardiac troponin I biomarker detection by aptamer-gold conjugates. ACS Omega **5**, 25899–25905.
22. Yola, M.L., and Atar, N. (2019). Development of cardiac troponin-I biosensor based on boron nitride quantum dots including molecularly imprinted polymer. Biosens. Bioelectron. **126**, 418–424.
23. El-Said, W.A., Fouad, D.M., and El-Safty, S.A. (2016). Ultrasensitive label-free detection of cardiac biomarker myoglobin based on surface-enhanced Raman spectroscopy. Sensor. Actuator. B Chem. **228**, 401–409.
24. Huang, D., Lin, B., Song, Y., et al. (2019). Staining traditional colloidal gold test strips with pt nanoshell enables quantitative point-of-care testing with simple and portable pressure meter readout. ACS Appl. Mater. Inter. **11**, 1800–1806.
25. Ji, T., Xu, X., Wang, X., et al. (2019). Point of care upconversion nanoparticles-based lateral flow assay quantifying myoglobin in clinical human blood samples. Sensor. Actuator. B Chem. **282**, 309–316.
26. Adeel, M., Rahman, M.M., and Lee, J.-J. (2019). Label-free aptasensor for the detection of cardiac biomarker myoglobin based on gold nanoparticles decorated boron nitride nanosheets. Biosens. Bioelectron. **126**, 143–150.
27. Zhu, L.-B., Lu, L., Wang, H.-Y., et al. (2019). Enhanced organic−inorganic heterojunction of polypyrrole@Bi2WO6: fabrication and application for sensitive photoelectrochemical immunoassay of creatine kinase-MB. Biosens. Bioelectron. **140**, 111349.
28. Lee, W.S., Sunkara, V., Han, J.-R., et al. (2015). Electrospun TiO2 nanofiber integrated lab-on-a-disc for ultrasensitive protein detection from whole blood. Lab Chip **15**, 478–485.

29. Wang, C., Li, J., Kang, M., et al. (2021). Nanodiamonds and hydrogen-substituted graphdiyne heteronanostructure for the sensitive impedimetric aptasensing of myocardial infarction and cardiac troponin I. Anal. Chim. Acta **1141**, 110−119.

30. Sun, Y., and Li, T. (2018). Composition-tunable hollow Au/Ag SERS nanoprobes coupled with target-catalyzed hairpin assembly for triple-amplification detection of miRNA. Anal. Chem. **90**, 11614−11621.

31. Sun, Y., Wang, Q., Mi, L., et al. (2019). Target-induced payload amplification for spherical nucleic acid enzyme (SNAzyme)-catalyzed electrochemiluminescence detection of circulating microRNAs. Anal. Chem. **91**, 12948−12953.

32. Mi, L., Sun, Y., Shi, L., et al. (2020). Hemin-bridged MOF interface with double amplification of g-quadruplex payload and DNAzyme catalysis: ultrasensitive lasting chemiluminescence microRNA imaging. ACS Appl. Mater. Inter. **12**, 7879−7887.

33. Shi, C., Xie, H., Ma, Y., et al. (2020). Nanoscale technologies in highly sensitive diagnosis of cardiovascular diseases. Front. Bioeng. Biotechnol. **8**, 531.

34. Surya, S.G., Majhi, S.M., Agarwal, D.K., et al. (2020). A label-free aptasensor FET based on Au nanoparticle decorated Co3O4 nanorods and a SWCNT layer for detection of cardiac troponin T protein. J. Mater. Chem. B **8**, 18−26.

35. Chi, H., Han, Q., Chi, T., et al. (2019). Manganese doped CdS sensitized graphene/Cu2MoS4 composite for the photoelectrochemical immunoassay of cardiac troponin I. Biosens. Bioelectron. **132**, 1−7.

36. Ma, Y., Dong, Y.-X., Wang, B., et al. (2020). CdS:Mn-sensitized 2D/2D heterostructured g-C3N4-MoS2 with excellent photoelectrochemical performance for ultrasensitive immunosensing platform. Talanta **207**, 120288.

37. Qin, X., Dong, Y., Wang, M., et al. (2018). C-dots assisted synthesis of gold nanoparticles as labels to catalyze copper deposition for ultrasensitive electrochemical sensing of proteins. Sci. China Chem. **61**, 476−482.

38. Singh, N., Rai, P., Ali, M.A., et al. (2019). A hollow-nanosphere-based microfluidic biosensor for biomonitoring of cardiac troponin I. J. Mater. Chem. B **7**, 3826−3839.

39. Supraja, P., Sudarshan, V., Tripathy, S., et al. (2019). Label free electrochemical detection of cardiac biomarker troponin T using ZnSnO3 perovskite nanomaterials. Anal. Methods **11**, 744−751.

40. Liyanage, T., Sangha, A., and Sardar, R. (2017). Achieving biosensing at attomolar concentrations of cardiac troponin T in human biofluids by developing a label-free nanoplasmonic analytical assay. Analyst **142**, 2442−2450.

41. Gupta, A., Sharma, S.K., Pachauri, V., et al. (2021). Sensitive impedimetric detection of troponin I with metal−organic framework composite electrode. RSC Adv. **11**, 2167−2174.

42. Yang, X., Yu, Y.-Q., Peng, L.-Z., et al. (2018). Strong electrochemiluminescence from MOF accelerator enriched quantum dots for enhanced sensing of trace cTnI. Anal. Chem. **90**, 3995−4002.

43. Hong, D., Jo, E.J., Kim, K., et al. (2020). Ru(bpy) 3 2+ -loaded mesoporous silica nanoparticles as electrochemiluminescent probes of a lateral flow immunosensor for highly sensitive and quantitative detection of Troponin I. Small **16**, 2004535.

44. Lim, W.Y., Thevarajah, T.M., Goh, B.T., et al. (2019). Paper microfluidic device for early diagnosis and prognosis of acute myocardial infarction via quantitative multiplex cardiac biomarker detection. Biosens. Bioelectron. **128**, 176−185.

45. Zhang, X., Lv, H., Li, Y., et al. (2019). Ultrasensitive sandwich-type immunosensor for cardiac troponin I based on enhanced electrocatalytic reduction of H2O2 using β-cyclodextrins functionalized 3D porous graphene-supported Pd@Au nanocubes. J. Mater. Chem. B **7**, 1460−1468.

46. Miao, L.Y., Jiao, L., Tang, Q.R., et al. (2019). A nanozyme-linked immunosorbent assay for dual-modal colorimetric and ratiometric fluorescent detection of cardiac troponin I. Sensor. Actuator. B Chem. **288**, 60−64.

47. Guo, X., Zong, L., Jiao, Y., et al. (2019). Signal-enhanced detection of multiplexed cardiac biomarkers by a paper-based fluorogenic immunodevice integrated with zinc oxide nanowires. Anal. Chem. **91**, 9300−9307.

48. Nechaeva, N.L., Sorokina, O.N., Konstantinova, T.S., et al. (2021). Simultaneous express immunoassay of multiple cardiac biomarkers with an automatic platform in human plasma. Talanta **224**, 121860.

49. Chen, X., and Liang, Y. (2021). Colorimetric sensing strategy for multiplexed detection of proteins based on three DNA-gold nanoparticle conjugates sensors. Sensor. Actuator. B Chem. **329**, 129202.

50. Xin, Y., Yang, R., Qu, Y., et al. (2020). Novel, highly sensitive, and specific assay to monitor acute myocardial infarction (AMI) by the determination of cardiac Troponin I (cTnI) and heart-type fatty acid binding protein (H-FABP) by a colloidal gold-based immunochromatographic test strip. Anal. Lett. **54**, 1329−1350.

51. Ji, J., Lu, W., Zhu, Y., et al. (2019). Porous hydrogel-encapsulated photonic barcodes for multiplex detection of cardiovascular biomarkers. ACS Sensors **4**, 1384−1390.

52. Singh, N., Ali, M.A., Rai, P., et al. (2020). Dual-modality microfluidic biosensor based on nanoengineered mesoporous graphene hydrogels. Lab Chip **20**, 760−777.

53. Shi, L., Sun, Y., Mi, L., et al. (2019). Target-catalyzed self-growing spherical nucleic acid enzyme (SNAzyme) as a double amplifier for ultrasensitive chemiluminescence microRNA detection. ACS Sensors **4**, 3219−3226.

54. Sun, Y., Shi, L., Wang, Q., et al. (2019). Spherical nucleic acid enzyme (SNAzyme) boosted chemiluminescence miRNA imaging using a smartphone. Anal. Chem. **91**, 3652−3658.

55. Cheng, T.M., Li, R., Kao, Y.C.J., et al. (2020). Synthesis and characterization of Gd-DTPA/fucoidan/peptide complex nanoparticle and in vitro magnetic resonance imaging of inflamed endothelial cells. Mater. Sci. Eng. C-Mater. Biol. Appl. **114**, 12.

56. Mateos, S., Lifante, J., Li, C.Y., et al. (2020). Instantaneous in vivo imaging of acute myocardial infarct by NIR-II luminescent nanodots. Small **16**, 10.

57. Woodard, P., Liu, Y., Pressly, E., et al. (2016). Design and modular construction of a polymeric nanoparticle for targeted atherosclerosis positron emission tomography imaging: a story of 25% (64)Cu-CANF-Comb. Pharm. Res. **33**, 2400−2410.

58. Liu, Y., Luehmann, H., Detering, L., et al. (2019). Assessment of targeted nanoparticle assemblies for atherosclerosis imaging with positron emission tomography and potential for clinical translation. ACS Appl. Mater. Inter. **11**, 15316−15321.

59. Xie, Z., Yang, Y., He, Y., et al. (2020). In vivo assessment of inflammation in carotid atherosclerosis by noninvasive photoacoustic imaging. Theranostics **10**, 4694−4704.

60. Guo, Z.D., Yang, L., Chen, M., et al. (2020). Molecular imaging of advanced atherosclerotic plaques with folate receptor-targeted 2D nanoprobes. Nano Res. **13**, 173−182.

61. Xu, J., Zhou, J., Zhong, Y., et al. (2017). Phase transition nanoparticles as multimodality contrast agents for the detection of thrombi and for targeting thrombolysis: in vitro and in vivo experiments. ACS Appl. Mater. Inter. **9**, 42525−42535.

62. Hu, J., Ortgies, D.H., Torres, R.A., et al. (2017). Quantum dots emitting in the third biological window as bimodal contrast agents for cardiovascular imaging. Adv. Funct. Mater. **27**, 9.

63. Liang, H.Y., Hong, Z.Z., Li, S.H., et al. (2021). An activatable X-ray scintillating luminescent nanoprobe for early diagnosis and progression monitoring of thrombosis in live rat. Adv. Funct. Mater. **31**, 10.

64. Dweck, M.R., Puntman, V., Vesey, A.T., et al. (2016). MR Imaging of coronary arteries and plaques. JACC Cardiovasc. Imag. **9**, 306−316.

65. Wüst, R.C.I., Calcagno, C., Daal, M.R.R., et al. (2019). Emerging magnetic resonance imaging techniques for atherosclerosis imaging. Arterioscler. Thromb. Vasc. Biol. **39**, 841−849.

66. Zhu, C., Sadat, U., Patterson, A.J., et al. (2014). 3D high-resolution contrast enhanced MRI of carotid atheroma−a technical update. Magn. Reson. Imag. **32**, 594−597.

67. Speelman, L., Teng, Z., Nederveen, A.J., et al. (2016). MRI-based biomechanical parameters for carotid artery plaque vulnerability assessment. Thromb. Haemost. **115**, 493−500.

68. Wei, Q., Wang, J., Shi, W., et al. (2019). Improved in vivo detection of atherosclerotic plaques with a tissue factor-targeting magnetic nanoprobe. Acta Biomater. **90**, 324−336.

69. Yu, M., Ortega, C.A., Si, K., et al. (2018). Nanoparticles targeting extra domain B of fibronectin-specific to the atherosclerotic lesion types III, IV, and V-enhance plaque detection and cargo delivery. Theranostics **8**, 6008−6024.

70. Qin, H., Zhou, T., Yang, S., et al. (2013). Gadolinium(III)-gold nanorods for MRI and photoacoustic imaging dual-modality detection of macrophages in atherosclerotic inflammation. Nanomedicine (Lond) **8**, 1611−1624.

71. Yu, M., Niu, Y., Zhou, D., et al. (2019). Hyaluronic acid-functionalized gadolinium doped iron oxide nanoparticles for atherosclerosis-targeted MR imaging. J. Biomed. Nanotechnol. **15**, 127−137.

72. Wang, J., Wu, M., Chang, J., et al. (2019). Scavenger receptor-AI-targeted ultrasmall gold nanoclusters facilitate in vivo MR and ex vivo fluorescence dual-modality visualization of vulnerable atherosclerotic plaques. Nanomedicine **19**, 81−94.

73. Montiel Schneider, M.G., and Lassalle, V.L. (2017). Magnetic iron oxide nanoparticles as novel and efficient tools for atherosclerosis diagnosis. Biomed. Pharmacother. **93**, 1098−1115.

74. Vazquez-Prada, K.X., Lam, J., Kamato, D., et al. (2020). Targeted molecular imaging of cardiovascular diseases by iron oxide nanoparticles. Arterioscler. Thromb. Vasc. Biol. **41**, 601−613.

75. Jacobin-Valat, M.J., Laroche-Traineau, J., Larivière, M., et al. (2015). Nanoparticles functionalised with an anti-platelet human antibody for in vivo detection of atherosclerotic plaque by magnetic resonance imaging. Nanomedicine **11**, 927−937.

76. Chen, J., Yang, J., Liu, R., et al. (2017). Dual-targeting theranostic system with mimicking apoptosis to promote myocardial infarction repair modulation of macrophages. Theranostics **7**, 4149−4167.

77. Poon, C., Gallo, J., Joo, J., et al. (2018). Hybrid, metal oxide-peptide amphiphile micelles for molecular magnetic resonance imaging of atherosclerosis. J. Nanobiotechnol. **16**, 11.

78. Zhang, S., Xu, W., Gao, P., et al. (2020). Construction of dual nanomedicines for the imaging and alleviation of atherosclerosis. Artif. Cell Nanomed. Biotechnol. **48**, 169−179.

79. Wei, X., Ying, M., Dehaini, D., et al. (2018). Nanoparticle functionalization with platelet membrane enables multifactored biological targeting and detection of atherosclerosis. ACS Nano **12**, 109−116.

80. Ye, S., Liu, Y., Lu, Y., et al. (2020). Cyclic RGD functionalized liposomes targeted to activated platelets for thrombosis dual-mode magnetic resonance imaging. J. Mater. Chem. B **8**, 447−453.

81. Narita, Y., Shimizu, K., Ikemoto, K., et al. (2019). Macrophage-targeted, enzyme-triggered fluorescence switch-on system for detection of embolism-vulnerable atherosclerotic plaques. J. Control. Release: Off. J. Control. Release Soc. **302**, 105−115.

82. Liang, M., Tan, H., Zhou, J., et al. (2018). Bioengineered H-Ferritin nanocages for quantitative imaging of vulnerable plaques in atherosclerosis. ACS Nano **12**, 9300−9308.

83. Ge, X., Cui, H., Kong, J., et al. (2020). A non-invasive nanoprobe for in vivo photoacoustic imaging of vulnerable atherosclerotic plaque. Adv. Mater. **32**, e2000037.

84. Li, L., Wang, J., Wu, M., et al. (2019). Macrophage-targeted and clearable glutathione-based MRI nanoprobes for atherosclerosis molecular imaging. J. Nanopart. Res. **21**, 231.

85. Tu, Y.F., Sun, Y., Fan, Y.H., et al. (2018). Multimodality molecular imaging of cardiovascular disease based on nanoprobes. Cell. Physiol. Biochem. **48**, 1401−1415.

86. Nahrendorf, M., Zhang, H., Hembrador, S., et al. (2008). Nanoparticle PET-CT imaging of macrophages in inflammatory atherosclerosis. Circulation **117**, 379−387.

87. Ta, H.T., Li, Z., Hagemeyer, C.E., et al. (2017). Molecular imaging of activated platelets via antibody-targeted ultrasmall iron oxide nanoparticles displaying unique dual MRI contrast. Biomaterials **134**, 31−42.

88. Mezzanotte, L., van 't Root, M., Karatas, H., et al. (2017). In vivo molecular bioluminescence imaging: new tools and applications. Trends Biotechnol. **35**, 640–652.

89. Osborn, E.A., and Jaffer, F.A. (2013). The advancing clinical impact of molecular imaging in CVD. JACC Cardiovasc. Imag. **6**, 1327–1341.

90. Douma, K., Megens, R., and van Zandvoort, M. (2011). Optical molecular imaging of atherosclerosis using nanoparticles: shedding new light on the darkness. Wiley Interdiscip. Rev. Nanomed. Nanobiotechnol. **3**, 376–388.

91. Mulder, W., Jaffer, F., Fayad, Z., et al. (2014). Imaging and nanomedicine in inflammatory atherosclerosis. Sci. Transl. Med. **6**, 239sr231.

92. Li, C., Chen, G., Zhang, Y., et al. (2020). Advanced fluorescence imaging technology in the near-infrared-II window for biomedical applications. J. Am. Chem. Soc. **142**, 14789–14804.

93. Huang, J., and Pu, K. (2020). Activatable molecular probes for second near-infrared fluorescence, chemiluminescence, and photoacoustic imaging. Angew. Chem. Int. Ed. Engl. **59**, 11717–11731.

94. Hu, Z., Fang, C., Li, B., et al. (2020). First-in-human liver-tumour surgery guided by multispectral fluorescence imaging in the visible and near-infrared-I/II windows. Nat. Biomed. Eng. **4**, 259–271.

95. Verjans, J.W., Osborn, E.A., Ughi, G.J., et al. (2016). Targeted near-infrared fluorescence imaging of atherosclerosis: clinical and intracoronary evaluation of indocyanine green. JACC Cardiovasc. Imag. **9**, 1087–1095.

96. Ughi, G.J., Wang, H., Gerbaud, E., et al. (2016). Clinical characterization of coronary atherosclerosis with dual-modality OCT and near-infrared autofluorescence imaging. JACC Cardiovasc. Imag. **9**, 1304–1314.

97. Beldman, T., Malinova, T., Desclos, E., et al. (2019). Nanoparticle-aided characterization of arterial endothelial architecture during atherosclerosis progression and metabolic therapy. ACS Nano **13**, 13759–13774.

98. Chen, H., Yuan, H., Cho, H., et al. (2017). Theranostic nucleic acid binding nanoprobe exerts anti-inflammatory and cytoprotective effects in ischemic injury. Theranostics **7**, 814–825.

99. Kwon, S.P., Jeon, S., Lee, S.H., et al. (2018). Thrombin-activatable fluorescent peptide incorporated gold nanoparticles for dual optical/computed tomography thrombus imaging. Biomaterials **150**, 125–136.

100. Zhou, H., Zeng, X., Li, A., et al. (2020). Upconversion NIR-II fluorophores for mitochondria-targeted cancer imaging and photothermal therapy. Nat. Commun. **11**, 6183.

101. Tian, R., Ma, H., Zhu, S., et al. (2020). Multiplexed NIR-II probes for lymph node-invaded cancer detection and imaging-guided surgery. Adv. Mater. **32**, e1907365.

102. Zhu, S., Tian, R., Antaris, A.L., et al. (2019). Near-Infrared-II molecular dyes for cancer imaging and surgery. Adv. Mater. **31**, e1900321.

103. Liu, H., Hong, G., Luo, Z., et al. (2019). Atomic-precision gold clusters for NIR-II imaging. Adv. Mater. **31**, e1901015.

104. Sun, X., Li, W., Zhang, X., et al. (2016). In vivo targeting and imaging of atherosclerosis using multifunctional virus-like particles of simian virus 40. Nano Lett. **16**, 6164–6171.

105. Jeong, S., Jung, Y., Bok, S., et al. (2018). Multiplexed in vivo imaging using size-controlled quantum dots in the second near-infrared window. Adv. Healthc. Mater. **7**, e1800695.

106. Gong, H., Peng, R., and Liu, Z. (2013). Carbon nanotubes for biomedical imaging: the recent advances. Adv. Drug Deliv. Rev. **65**, 1951–1963.

107. Robinson, J.T., Hong, G., Liang, Y., et al. (2012). In vivo fluorescence imaging in the second near-infrared window with long circulating carbon nanotubes capable of ultrahigh tumor uptake. J. Am. Chem. Soc. **134**, 10664–10669.

108. Qiao, R.R., Qiao, H.Y., Zhang, Y., et al. (2017). Molecular imaging of vulnerable atherosclerotic plaques in vivo with osteopontin-specific upconversion nanoprobes. Acs Nano **11**, 1816–1825.

109. Liu, B., Li, C., Yang, P., et al. (2017). 808-nm-light-excited lanthanide-doped nanoparticles: rational design, luminescence control and theranostic applications. Adv. Mater. **29**, 1605434.

110. Labrador-Páez, L., Ximendes, E.C., Rodríguez-Sevilla, P., et al. (2018). Core-shell rare-earth-doped nanostructures in biomedicine. Nanoscale **10**, 12935–12956.

111. Andrews, J.P.M., Fayad, Z.A., and Dweck, M.R. (2018). New methods to image unstable atherosclerotic plaques. Atherosclerosis **272**, 118–128.

112. Nie, X., Laforest, R., Elvington, A., et al. (2016). PET/MRI of hypoxic atherosclerosis using 64Cu-ATSM in a rabbit model. J. Nucl. Med. **57**, 2006–2011.

113. Tarkin, J.M., Joshi, F.R., and Rudd, J.H. (2014). PET imaging of inflammation in atherosclerosis. Nat. Rev. Cardiol. **11**, 443–457.

114. Joshi, N.V., Vesey, A.T., Williams, M.C., et al. (2014). 18F-fluoride positron emission tomography for identification of ruptured and high-risk coronary atherosclerotic plaques: a prospective clinical trial. Lancet **383**, 705–713.

115. Luehmann, H., Detering, L., Fors, B., et al. (2016). PET/CT Imaging of chemokine receptors in inflammatory atherosclerosis using targeted nanoparticles. J. Nucl. Med.: Off. Publ. Soc. Nucl. Med. **57**, 1124–1129.

116. White, G., Iqbal, A., and Greaves, D. (2013). CC chemokine receptors and chronic inflammation—therapeutic opportunities and pharmacological challenges. Pharmacol. Rev. **65**, 47–89.

117. Zernecke, A., Shagdarsuren, E., and Weber, C. (2008). Chemokines in atherosclerosis: an update. Arterioscler. Thromb. Vasc. Biol. **28**, 1897–1908.

118. Zhao, Y., Liang, M., Li, X., et al. (2016). Bioengineered magnetoferritin nanoprobes for single-dose nuclear-magnetic resonance tumor imaging. ACS Nano **10**, 4184–4191.

119. Casco, V., Veinot, J., Kuroski de Bold, M., et al. (2002). Natriuretic peptide system gene expression in human coronary arteries. J. Histochem. Cytochem.: Off. J. Histochem. Soc. **50**, 799–809.

120. Liu, Y., Abendschein, D., Woodard, G., et al. (2010). Molecular imaging of atherosclerotic plaque with (64)Cu-labeled natriuretic peptide and PET. J. Nucl. Med.: Off. Publ. Soc. Nucl. Med. **51**, 85–91.

121. Fernández-Friera, L., Fuster, V., López-Melgar, B., et al. (2019). Vascular inflammation in subclinical atherosclerosis detected by hybrid PET/MRI. J. Am. Coll. Cardiol. **73**, 1371–1382.

122. Senders, M.L., Hernot, S., Carlucci, G., et al. (2019). Nanobody-facilitated multiparametric PET/MRI phenotyping of atherosclerosis. JACC Cardiovasc. Imag. **12**, 2015–2026.

123. Li, Y., Pan, Y., Wu, X., et al. (2019). Dual-modality imaging of atherosclerotic plaques using ultrasmall superparamagnetic iron oxide labeled with rhodamine. Nanomedicine (Lond) **14**, 1935–1944.

124. Yao, Y., Li, B., Yin, C., et al. (2016). A folate-conjugated dual-modal fluorescent magnetic resonance imaging contrast agent that targets activated macrophages in vitro and in vivo. J. Biomed. Nanotechnol. **12**, 2161–2171.

125. Pérez-Medina, C., Binderup, T., Lobatto, M., et al. (2016). In vivo PET imaging of HDL in multiple atherosclerosis models. JACC Cardiovasc. Imag. **9**, 950–961.

126. Song, Y., Huang, Z., Xu, J., et al. (2014). Multimodal SPION-CREKA peptide based agents for molecular imaging of microthrombus in a rat myocardial ischemia-reperfusion model. Biomaterials **35**, 2961–2970.

127. Keliher, E.J., Ye, Y.X., Wojtkiewicz, G.R., et al. (2017). Polyglucose nanoparticles with renal elimination and macrophage avidity facilitate PET imaging in ischaemic heart disease. Nat. Commun. **8**, 12.

128. Beldman, T., Senders, M., Alaarg, A., et al. (2017). Hyaluronan nanoparticles selectively target plaque-associated macrophages and improve plaque stability in atherosclerosis. ACS Nano **11**, 5785–5799.

129. Pellico, J., Fernandez-Barahona, I., Benito, M., et al. (2019). Unambiguous detection of atherosclerosis using bioorthogonal nanomaterials. Nanomed. Nanotechnol. Biol. Med. **17**, 26–35.

130. Su, T., Wang, Y.B., Han, D., et al. (2017). Multimodality imaging of angiogenesis in a rabbit atherosclerotic model by GEBP11 peptide targeted nanoparticles. Theranostics **7**, 4791–4804.

131. Senders, M.L., Meerwaldt, A.E., van Leent, M.M.T., et al. (2020). Probing myeloid cell dynamics in ischaemic heart disease by nanotracer hot-spot imaging. Nat. Nanotechnol. **15**, 398–405.

132. Li, Y., Xin, F., Hu, J., et al. (2020). Functionalization of NaGdF4 nanoparticles with a dibromomaleimide-terminated polymer for MR/optical imaging of thrombosis. Polym. Chem. **11**, 1010–1017.

133. Wang, Y., Zhang, Y., Wang, Z., et al. (2019). Optical/MRI dual-modality imaging of M1 macrophage polarization in atherosclerotic plaque with MARCO-targeted upconversion luminescence probe. Biomaterials **219**, 119378.

134. Larivière, M., Lorenzato, C., Adumeau, L., et al. (2019). Multimodal molecular imaging of atherosclerosis: nanoparticles functionalized with scFv fragments of an anti-αIIbβ3 antibody. Nanomed. Nanotechnol. Biol. Med. **22**, 102082.

135. Zheng, Y., Zhang, H., Hu, Y., et al. (2018). MnO nanoparticles with potential application in magnetic resonance imaging and drug delivery for myocardial infarction. Int. J. Nanomed. **13**, 6177–6188.

136. Kao, C.W., Wu, P.T., Liao, M.Y., et al. (2018). Magnetic nanoparticles conjugated with peptides derived from monocyte chemoattractant protein-1 as a tool for targeting atherosclerosis. Pharmaceutics **10**, 17.

137. Qiao, H., Wang, Y., Zhang, R., et al. (2017). MRI/optical dual-modality imaging of vulnerable atherosclerotic plaque with an osteopontin-targeted probe based on Fe(3)O(4) nanoparticles. Biomaterials **112**, 336–345.

138. Wang, Y., Chen, J., Yang, B., et al. (2016). In vivo MR and fluorescence dual-modality imaging of atherosclerosis characteristics in mice using profilin-1 targeted magnetic nanoparticles. Theranostics **6**, 272–286.

139. Jung, E., Kang, C., Lee, J., et al. (2018). Molecularly engineered theranostic nanoparticles for thrombosed vessels: H2O2-activatable contrast-enhanced photoacoustic imaging and antithrombotic therapy. ACS Nano **12**, 392–401.

140. Steinberg, I., Huland, D.M., Vermesh, O., et al. (2019). Photoacoustic clinical imaging. Photoacoustics **14**, 77–98.

141. Gao, W., Sun, Y., Cai, M., et al. (2018). Copper sulfide nanoparticles as a photothermal switch for TRPV1 signaling to attenuate atherosclerosis. Nat. Commun. **9**, 231.

142. Qin, H., Zhao, Y., Zhang, J., et al. (2016). Inflammation-targeted gold nanorods for intravascular photoacoustic imaging detection of matrix metalloproteinase-2 (MMP(2)) in atherosclerotic plaques. Nanomedicine **12**, 1765–1774.

143. Qin, J., Peng, Z., Li, B., et al. (2015). Gold nanorods as a theranostic platform for in vitro and in vivo imaging and photothermal therapy of inflammatory macrophages. Nanoscale **7**, 13991–14001.

144. Qin, H., Zhou, T., Yang, S., et al. (2015). Fluorescence quenching nanoprobes dedicated to in vivo photoacoustic imaging and high-efficient tumor therapy in deep-seated tissue. Small **11**, 2675–2686.

145. Jung, E., Lee, J., Jeong, L., et al. (2019). Stimulus-activatable echogenic maltodextrin nanoparticles as nanotheranostic agents for peripheral arterial disease. Biomaterials **192**, 282–291.

146. Kang, C., Gwon, S., Song, C., et al. (2017). Fibrin-targeted and H2O2-responsive nanoparticles as a theranostics for thrombosed vessels. ACS Nano **11**, 6194–6203.

147. Chaudhary, R., Roy, K., Kanwar, R., et al. (2016). Engineered atherosclerosis-specific zinc ferrite nanocomplex-based MRI contrast agents. J. Nanobiotechnol. **14**, 6.

148. Hossaini Nasr, S., Rashidijahanabad, Z., Ramadan, S., et al. (2020). Effective atherosclerotic plaque inflammation inhibition with targeted drug delivery by hyaluronan conjugated atorvastatin nanoparticles. Nanoscale *12*, 9541–9556.

149. Gao, C., Huang, Q., Liu, C., et al. (2020). Treatment of atherosclerosis by macrophage-biomimetic nanoparticles via targeted pharmacotherapy and sequestration of proinflammatory cytokines. Nat. Commun. *11*, 2622.

150. Boada, C., Zinger, A., Tsao, C., et al. (2020). Rapamycin-loaded biomimetic nanoparticles reverse vascular inflammation. Circ. Res. *126*, 25–37.

151. Qiu, J., Cai, G., Liu, X., et al. (2017). α(v)β(3) integrin receptor specific peptide modified, salvianolic acid B and panax notoginsenoside loaded nanomedicine for the combination therapy of acute myocardial ischemia. Biomed. Pharmacother. *96*, 1418–1426.

152. Lameijer, M., Binderup, T., van Leent, M., et al. (2018). Efficacy and safety assessment of a TRAF6-targeted nanoimmunotherapy in atherosclerotic mice and non-human primates. Nat. Biomed. Eng. *2*, 279–292.

153. Seijkens, T., van Tiel, C., Kusters, P., et al. (2018). Targeting CD40-Induced TRAF6 signaling in macrophages reduces atherosclerosis. J. Am. Coll. Cardiol. *71*, 527–542.

154. Rink, J.S., Sun, W., Misener, S., et al. (2018). Nitric oxide-delivering high-density lipoprotein-like nanoparticles as a biomimetic nanotherapy for vascular diseases. ACS Appl. Mater. Inter. *10*, 6904–6916.

155. Tao, W., Yurdagul, A., Kong, N., et al. (2020). siRNA nanoparticles targeting CaMKIIγ in lesional macrophages improve atherosclerotic plaque stability in mice. Sci. Transl. Med. *12*, eaay1063.

156. Chin, D.D., Poon, C., Wang, J., et al. (2021). miR-145 micelles mitigate atherosclerosis by modulating vascular smooth muscle cell phenotype. Biomaterials *273*, 120810.

157. Lockhart, J.H., VanWye, J., Banerjee, R., et al. (2021). Self-assembled miRNA-switch nanoparticles target denuded regions and prevent restenosis. Mol. Ther. *29*, 1744–1757.

158. Liao, J., and Laufs, U. (2005). Pleiotropic effects of statins. Annu. Rev. Pharmacol. Toxicol. *45*, 89–118.

159. Armitage, J. (2007). The safety of statins in clinical practice. Lancet *370*, 1781–1790.

160. Wang, Y., Zhang, K., Li, T., et al. (2021). Macrophage membrane functionalized biomimetic nanoparticles for targeted anti-atherosclerosis application. Theranostics *11*, 164–180.

161. Kim, H., Kumar, S., Kang, D.W., et al. (2020). Affinity-driven design of cargo-switching nanoparticles to leverage a cholesterol-rich microenvironment for atherosclerosis therapy. ACS Nano *14*, 6519–6531.

162. Wang, Y., Zhang, K., Qin, X., et al. (2019). Biomimetic nanotherapies: red blood cell based core-shell structured nanocomplexes for atherosclerosis management. Adv. Sci. (Weinheim, Baden-Wurttemberg, Germany) *6*, 1900172.

163. Wang, B., Chen, G., Urabe, G., et al. (2018). A paradigm of endothelium-protective and stent-free anti-restenotic therapy using biomimetic nanoclusters. Biomaterials *178*, 293–301.

164. Toole, B.P. (2004). Hyaluronan: from extracellular glue to pericellular cue. Nat. Rev. Cancer *4*, 528–539.

165. Choisnard, L., Gèze, A., Putaux, J.L., et al. (2006). Nanoparticles of beta-cyclodextrin esters obtained by self-assembling of biotransesterified beta-cyclodextrins. Biomacromolecules *7*, 515–520.

166. Kurdi, A., Martinet, W., and De Meyer, G.R.Y. (2018). mTOR inhibition and cardiovascular diseases: dyslipidemia and atherosclerosis. Transplantation *102*, s44–s46.

167. Weber, C., and Noels, H. (2011). Atherosclerosis: current pathogenesis and therapeutic options. Nat. Med. *17*, 1410–1422.

168. Colombo, A., Drzewiecki, J., Banning, A., et al. (2003). Randomized study to assess the effectiveness of slow- and moderate-release polymer-based paclitaxel-eluting stents for coronary artery lesions. Circulation *108*, 788–794.

169. Fava, C., and Montagnana, M. (2018). Atherosclerosis is an inflammatory disease which lacks a common anti-inflammatory therapy: how human genetics can help to this issue. a narrative review. Front. Pharmacol. *9*, 55.

170. Dong, Y., Chen, H., Chen, C., et al. (2016). Polymer-lipid hybrid theranostic nanoparticles co-delivering ultrasmall superparamagnetic iron oxide and paclitaxel for targeted magnetic resonance imaging and therapy in atherosclerotic plaque. J. Biomed. Nanotechnol. *12*, 1245–1257.

171. Williams, K., and Tabas, I. (1999). Atherosclerosis–an inflammatory disease. New Engl. J. Med. *340*, 1928–1929.

172. Martinez, J.O., Molinaro, R., Hartman, K.A., et al. (2018). Biomimetic nanoparticles with enhanced affinity towards activated endothelium as versatile tools for theranostic drug delivery. Theranostics *8*, 1131–1145.

173. Song, Y., Huang, Z., Liu, X., et al. (2019). Platelet membrane-coated nanoparticle-mediated targeting delivery of rapamycin blocks atherosclerotic plaque development and stabilizes plaque in apolipoprotein E-deficient (ApoE(-/-)) mice. Nanomedicine *15*, 13–24.

174. Gao, M., Liang, C., Song, X., et al. (2017). Erythrocyte-membrane-enveloped perfluorocarbon as nanoscale artificial red blood cells to relieve tumor hypoxia and enhance cancer radiotherapy. Adv. Mater. *29*, 1701429.

175. Zhang, L., Wang, Z., Zhang, Y., et al. (2018). Erythrocyte membrane cloaked metal-organic framework nanoparticle as biomimetic nanoreactor for starvation-activated colon cancer therapy. ACS Nano *12*, 10201–10211.

176. Stone, G., Moses, J., Ellis, S., et al. (2007). Safety and efficacy of sirolimus- and paclitaxel-eluting coronary stents. New Engl. J. Med. *356*, 998–1008.

177. Stefanini, G.G., and Holmes, D.R., Jr. (2013). Drug-eluting coronary-artery stents. N. Engl. J. Med. *368*, 254–265.

178. Betala, J., Bae, S., Langan, E., et al. (2020). Ex vivo combinatorial therapy of sirolimus and heparin by nanocarrier inhibits restenosis after balloon angioplasty. Nanomedicine (London, England) *15*, 1205–1220.

179. Feng, S., Hu, Y., Peng, S., et al. (2016). Nanoparticles responsive to the inflammatory microenvironment for targeted treatment of arterial restenosis. Biomaterials *105*, 167–184.

180. Dou, Y., Chen, Y., Zhang, X., et al. (2017). Non-proinflammatory and responsive nanoplatforms for targeted treatment of atherosclerosis. Biomaterials *143*, 93–108.

181. Zhu, X., Xie, H., Liang, X., et al. (2017). Bilayered nanoparticles with sequential release of VEGF gene and paclitaxel for restenosis inhibition in atherosclerosis. ACS Appl. Mater. Inter. *9*, 27522–27532.

182. Swirski, F.K., and Nahrendorf, M. (2013). Leukocyte behavior in atherosclerosis, myocardial infarction, and heart failure. Science *339*, 161–166.

183. Wynn, T.A., Chawla, A., and Pollard, J.W. (2013). Macrophage biology in development, homeostasis and disease. Nature *496*, 445–455.

184. Tang, J., Baxter, S., Menon, A., et al. (2016). Immune cell screening of a nanoparticle library improves atherosclerosis therapy. Proc. Natl. Acad. Sci. U S A *113*, E6731–E6740.

185. Yu, M., Amengual, J., Menon, A., et al. (2017). Targeted nanotherapeutics encapsulating liver X receptor agonist GW3965 enhance antiatherogenic effects without adverse effects on hepatic lipid metabolism in Ldlr(-/-) mice. Adv. Healthc. Mater. *6*, 1700313.

186. Fujiwara, M., Matoba, T., Koga, J., et al. (2019). Nanoparticle incorporating Toll-like receptor 4 inhibitor attenuates myocardial ischaemia-reperfusion injury by inhibiting monocyte-mediated inflammation in mice. Cardiovasc. Res. *115*, 1244–1255.

187. Tokutome, M., Matoba, T., Nakano, Y., et al. (2019). Peroxisome proliferator-activated receptor-gamma targeting nanomedicine promotes cardiac healing after acute myocardial infarction by skewing monocyte/macrophage polarization in preclinical animal models. Cardiovasc. Res. *115*, 419–431.

188. Lee, I.H., Cao, L., Mostoslavsky, R., et al. (2008). A role for the NAD-dependent deacetylase Sirt1 in the regulation of autophagy. Proc. Natl. Acad. Sci. U S A *105*, 3374–3379.

189. Ma, S., Motevalli, S., Chen, J., et al. (2018). Precise theranostic nanomedicines for inhibiting vulnerable atherosclerotic plaque progression through regulation of vascular smooth muscle cell phenotype switching. Theranostics *8*, 3693–3706.

190. Yu, L., Li, S., Tang, X., et al. (2017). Diallyl trisulfide ameliorates myocardial ischemia-reperfusion injury by reducing oxidative stress and endoplasmic reticulum stress-mediated apoptosis in type 1 diabetic rats: role of SIRT1 activation. Apoptosis: Int. J. Program. Cell Death *22*, 942–954.

191. Karwi, Q., Bice, J., and Baxter, G. (2018). Pre- and postconditioning the heart with hydrogen sulfide (HS) against ischemia/reperfusion injury in vivo: a systematic review and meta-analysis. Basic Res. Cardiol. *113*, 6.

192. Wang, W., Liu, H., Lu, Y., et al. (2019). Controlled-releasing hydrogen sulfide donor based on dual-modal iron oxide nanoparticles protects myocardial tissue from ischemia-reperfusion injury. Int. J. Nanomed. *14*, 875–888.

193. Hao, P., Jiang, F., Cheng, J., et al. (2017). Traditional Chinese medicine for cardiovascular disease: evidence and potential mechanisms. J. Am. Coll. Cardiol. *69*, 2952–2966.

194. Jiang, L., Wang, J., Jiang, J., et al. (2020). Sonodynamic therapy in atherosclerosis by curcumin nanosuspensions: preparation design, efficacy evaluation, and mechanisms analysis. Eur. J. Pharm. Biopharm.: Off. J. Arbeitsgemeinschaft Pharm. Verfahrenstech. e.V *146*, 101–110.

195. Hassanzadeh, K., Buccarello, L., Dragotto, J., et al. (2020). Obstacles against the marketing of curcumin as a drug. Int. J. Mol. Sci. *21*, 6619.

196. Ibrar, M., Khan, M., Abdullah, et al. (2018). Evaluation of paeonia emodi and its gold nanoparticles for cardioprotective and antihyperlipidemic potentials. J. Photochem. Photobiol. B Biol. *189*, 5–13.

197. Jiang, J., Yuan, X., Wang, T., et al. (2014). Antioxidative and cardioprotective effects of total flavonoids extracted from Dracocephalum moldavica L. against acute ischemia/reperfusion-induced myocardial injury in isolated rat heart. Cardiovasc. Toxicol. *14*, 74–82.

198. Tan, M., He, C., Jiang, W., et al. (2017). Development of solid lipid nanoparticles containing total flavonoid extract from Dracocephalum moldavica L. and their therapeutic effect against myocardial ischemia-reperfusion injury in rats. Int. J. Nanomed. *12*, 3253–3265.

199. Kim, M., Sahu, A., Hwang, Y., et al. (2020). Targeted delivery of anti-inflammatory cytokine by nanocarrier reduces atherosclerosis in Apo E(-/-) mice. Biomaterials *226*, 119550.

200. Wang, X., Gkanatsas, Y., Palasubramaniam, J., et al. (2016). Thrombus-targeted theranostic microbubbles: a new technology towards concurrent rapid ultrasound diagnosis and bleeding-free fibrinolytic treatment of thrombosis. Theranostics *6*, 726–738.

201. Yang, T., Ding, X., Dong, L., et al. (2018). Platelet-mimic uPA delivery nanovectors based on Au rods for thrombus targeting and treatment. ACS Biomater. Sci. Eng. *4*, 4219–4224.

202. Pawlowski, C., Li, W., Sun, M., et al. (2017). Platelet microparticle-inspired clot-responsive nanomedicine for targeted fibrinolysis. Biomaterials *128*, 94–108.

203. Tyler, B., Gullotti, D., Mangraviti, A., et al. (2016). Polylactic acid (PLA) controlled delivery carriers for biomedical applications. Adv. Drug Del. Rev. *107*, 163–175.

204. Devel, L., Almer, G., Cabella, C., et al. (2019). Biodistribution of nanostructured lipid carriers in mice atherosclerotic model. Molecules (Basel, Switzerland) *24*, 3499.

205. Ramirez-Carracedo, R., Tesoro, L., Hernandez, I., et al. (2018). Non-invasive detection of extracellular matrix metalloproteinase inducer EMMPRIN, a new therapeutic target against atherosclerosis, inhibited by endothelial nitric oxide. Int. J. Mol. Sci. *19*, 3248.

206. Kamaly, N., Fredman, G., Fojas, J.J., et al. (2016). Targeted interleukin-10 nanotherapeutics developed with a microfluidic chip enhance resolution of inflammation in advanced atherosclerosis. ACS Nano *10*, 5280–5292.

207. Tadin-Strapps, M., Robinson, M., Le Voci, L., et al. (2015). Development of lipoprotein(a) siRNAs for mechanism of action studies in non-human primate models of atherosclerosis. J. Cardiovasc. Transl. Res. *8*, 44–53.

208. Chi, X., Gatti, P., and Papoian, T. (2017). Safety of antisense oligonucleotide and siRNA-based therapeutics. Drug Discov. Today *22*, 823–833.

209. Thenmozhi, R., Lee, J.S., Park, N.Y., et al. (2020). Gene therapy options as new treatment for inherited peripheral neuropathy. Exp. Neurobiol. **29**, 177–188.

210. Pan, H., Palekar, R.U., Hou, K.K., et al. (2018). Anti-JNK2 peptide-siRNA nanostructures improve plaque endothelium and reduce thrombotic risk in atherosclerotic mice. Int. J. Nanomed. **13**, 5187–5205.

211. Sager, H., Dutta, P., Dahlman, J., et al. (2016). RNAi targeting multiple cell adhesion molecules reduces immune cell recruitment and vascular inflammation after myocardial infarction. Sci. Transl. Med. **8**, 342ra380.

212. Khan, O.F., Kowalski, P.S., Doloff, J.C., et al. (2018). Endothelial siRNA delivery in nonhuman primates using ionizable low-molecular weight polymeric nanoparticles. Sci. Adv. **4**, eaar8409.

213. Jiang, C., Qi, Z., Jia, H., et al. (2019). ATP-responsive low-molecular-weight polyethylenimine-based supramolecular assembly via host-guest interaction for gene delivery. Biomacromolecules **20**, 478–489.

214. Jiang, C., Qi, Z., He, W., et al. (2019). Dynamically enhancing plaque targeting via a positive feedback loop using multifunctional biomimetic nanoparticles for plaque regression. J. Control. Release: Off. J. Control. Release Soc. **308**, 71–85.

215. Nguyen, M.A., Wyatt, H., Susser, L., et al. (2019). Delivery of microRNAs by chitosan nanoparticles to functionally alter macrophage cholesterol efflux in vitro and in vivo. ACS Nano **13**, 6491–6505.

216. Huang, C.K., Kafert-Kasting, S., and Thum, T. (2020). Preclinical and clinical development of noncoding RNA therapeutics for cardiovascular disease. Circ. Res. **126**, 663–678.

217. Lucas, T., Bonauer, A., and Dimmeler, S. (2018). RNA therapeutics in cardiovascular disease. Circ. Res. **123**, 205–220.

218. Sayed, N., Tambe, P., Kumar, P., et al. (2020). miRNA transfection via poly(amidoamine)-based delivery vector prevents hypoxia/reperfusion-induced cardiomyocyte apoptosis. Nanomedicine (London, England) **15**, 163–181.

219. Ling, H., Fabbri, M., and Calin, G.A. (2013). microRNAs and other non-coding RNAs as targets for anticancer drug development. Nat. Rev. Drug Discov. **12**, 847–865.

220. Liu, F., Ding, N., Huo, D., et al. (2019). Surface-engineered monocyte inhibits atherosclerotic plaque destabilization via graphene quantum dot-mediated microRNA delivery. Adv. Healthc. Mater. **8**, e1900386.

221. Lu, J., Zhao, Y., Zhou, X., et al. (2017). Biofunctional polymer-lipid hybrid high-density lipoprotein-mimicking nanoparticles loading anti-miR155 for combined antiatherogenic effects on macrophages. Biomacromolecules **18**, 2286–2295.

222. Lockhart, J., Canfield, J., Mong, E.F., et al. (2019). Nucleotide modification alters microRNA-dependent silencing of microRNA switches. Mol. Ther. Nucleic Acids **14**, 339–350.

223. Wang, Y., Li, L., Zhao, W., et al. (2018). Targeted therapy of atherosclerosis by a broad-spectrum reactive oxygen species scavenging nanoparticle with intrinsic anti-inflammatory activity. ACS Nano **12**, 8943–8960.

224. Liu, H., Xu, H., and Huang, K. (2017). Selenium in the prevention of atherosclerosis and its underlying mechanisms. Metallomics **9**, 21–37.

225. Benstoem, C., Goetzenich, A., Kraemer, S., et al. (2015). Selenium and its supplementation in cardiovascular disease—what do we know? Nutrients **7**, 3094–3118.

226. Maiyo, F., and Singh, M. (2017). Selenium nanoparticles: potential in cancer gene and drug delivery. Nanomedicine (Lond) **12**, 1075–1089.

227. Meng, Y., Zhang, Y., Jia, N., et al. (2018). Synthesis and evaluation of a novel water-soluble high Se-enriched astragalus polysaccharide nanoparticles. Int. J. Biol. Macromol. **118**, 1438–1448.

228. Guo, L., Xiao, J., Liu, H., et al. (2020). Selenium nanoparticles alleviate hyperlipidemia and vascular injury in ApoE-deficient mice by regulating cholesterol metabolism and reducing oxidative stress. Metallomics **12**, 204–217.

229. Shrivastava, S., Bera, T., Singh, S., et al. (2009). Characterization of antiplatelet properties of silver nanoparticles. ACS Nano **3**, 1357–1364.

230. Ojo, S., Lateef, A., Azeez, M., et al. (2016). Biomedical and catalytic applications of gold and silver-gold alloy nanoparticles biosynthesized using cell-free extract of bacillus safensis LAU 13: antifungal, dye degradation, anti-coagulant and thrombolytic activities. IEEE Trans. Nanobiosci. **15**, 433–442.

231. Han, X., Li, H., Jiang, Y., et al. (2017). Upconversion nanoparticle-mediated photodynamic therapy induces autophagy and cholesterol efflux of macrophage-derived foam cells via ROS generation. Cell Death Dis. **8**, e2864.

232. Vonnemann, J., Beziere, N., Böttcher, C., et al. (2014). Polyglycerolsulfate functionalized gold nanorods as optoacoustic signal nanoamplifiers for in vivo bioimaging of rheumatoid arthritis. Theranostics **4**, 629–641.

233. Yong, J., Needham, K., Brown, W., et al. (2014). Gold-nanorod-assisted near-infrared stimulation of primary auditory neurons. Adv. Healthc. Mater. **3**, 1862–1868.

234. Wang, X., Wu, X., Qin, J., et al. (2019). Differential phagocytosis-based photothermal ablation of inflammatory macrophages in atherosclerotic disease. ACS Appl. Mater. Inter. **11**, 41009–41018.

235. Zhang, F., Liu, Y., Lei, J., et al. (2019). Metal-organic-framework-derived carbon nanostructures for site-specific dual-modality photothermal/photodynamic thrombus therapy. Adv. Sci. (Weinheim, Baden-Wurttemberg, Germany) **6**, 1901378.

236. Guo, S., Guo, X., Wang, X., et al. (2019). Reduced clot debris size in sonothrombolysis assisted with phase-change nanodroplets. Ultrason. Sonochem. **54**, 183–191.

237. Yang, W., and Zhou, Y. (2017). Effect of pulse repetition frequency of high-intensity focused ultrasound on in vitro thrombolysis. Ultrason. Sonochem. **35**, 152–160.

238. Zhong, Y., Zhang, Y., Xu, J., et al. (2019). Low-intensity focused ultrasound-responsive phase-transitional nanoparticles for thrombolysis without vascular damage: a synergistic nonpharmaceutical strategy. ACS Nano **13**, 3387–3403.

239. Wu, Y., Zhang, R., Tran, H.D.N., et al. (2021). Chitosan nanococktails containing both ceria and superparamagnetic iron oxide nanoparticles for reactive oxygen species-related theranostics. ACS Appl. Nano Mater. **4**, 3604–3618.

240. Wang, Y., Xu, X., Zhao, X., et al. (2021). Functionalized polymeric hybrid micelles as an efficient nanotheranostic agent for thrombus imaging and thrombolysis. Acta Biomater. **122**, 278–290.

241. Binderup, T., Duivenvoorden, R., Fay, F., et al. (2019). Imaging-assisted nanoimmunotherapy for atherosclerosis in multiple species. Sci. Transl. Med. **11**, 506.

ACKNOWLEDGMENTS

AUTHOR CONTRIBUTIONS

H.L. and J.G. proposed the conception, study design, and had the final approval of the manuscript submitted. Q.H. and Z.F. participated in the data collections and analysis, the drafting of the manuscript, and the submission.

DECLARATION OF INTERESTS

The authors declare no competing interests.

SUPPLEMENTAL INFORMATION

Supplemental information can be found online at https://doi.org/10.1016/j.xinn.2022.100214.